HELLENIC REPUBLIC
National and Kapodistrian University of Athens
EST. 1837

"ALEXANDER FLEMING"
Biomedical Sciences Research Center

NATIONAL AND KAPODISTRIAN UNIVERSITY OF ATHENS,
MEDICAL SCHOOL

"Studying the pro-tumorigenic role of IGF1 in muscle-invasive urinary bladder cancer"

Christina Paraskeva

Supervisor: Vasiliki Koliaraki, Researcher B', BSCR "Alexander Fleming"

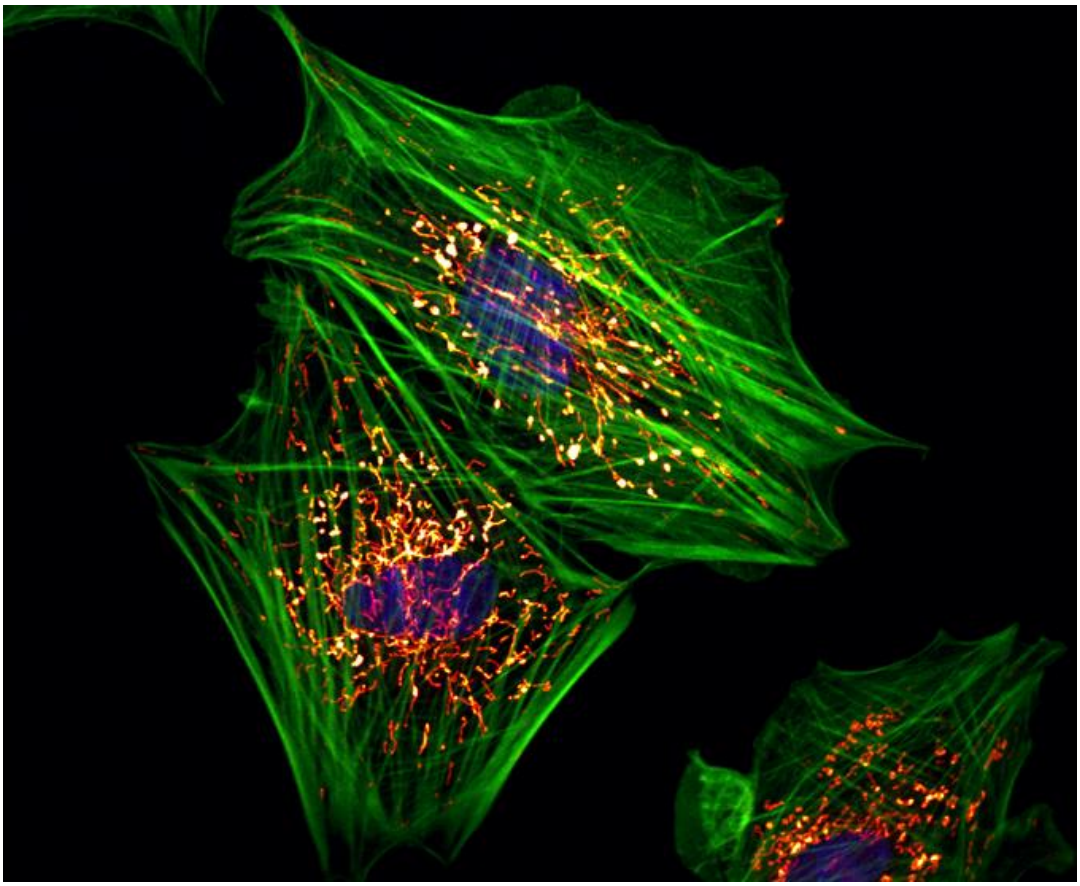

MOLECULAR BIOMEDICINE: Mechanisms of Disease, Molecular And Cellular Therapies And Bioinnovation

June 2022

Table of contents

Abbreviations	
Abbreviation	**Definition**
ARG	Arginase
ALS	Acid Labile Subunit
a-SMA	alpha-Smooth Muscle Actin
BAD	Bcl2 Associated agonist of cell Death
BCL2	B-Cell Lymphoma-2
CAF	Cancer Associated Fibroblast
CAV1	Caveolin-1
CIS	Carcinoma in situ
CNS	Central Nervous System
DAMPs	Damage Associated Molecular Patterns
DNMT3B	DNA Methyltransferase 3B
ECM	Extracellular Matrix
EGFR	Epidermal Growth Factor Receptor
EMT	Epithelial to Mesenchymal Transition
EndoMT	Endothelial to Mesenchymal Transition
Erβ	Estrogen Receptor β
FAF	Fibrosis Associated Fibroblast
FAP	Fibroblast Activation Protein
FSP1	Fibroblast Specific Protein-1
GAS6	Growth Arrest Specific protein-6
GDF15	Growth Differentiation Factor-5
GH	Growth Hormone
GHrH	Growth Hormone releasing Hormone
GSK3β	Glycogen Synthase Kinase-3 beta
HSF-1	Heat Shock Factor 1
IDO1	Indoleamine 2,3 dioxygenase-1
IGF	Insulin-like Growth Factor
IGFBP	Insulin-like Growth Factor Binding Protein
InsR	Insulin Receptor
IR	Insulin Receptor
IRS	Insulin Receptor Substrate
LIF	Leukemia Inhibitor Factor

MAPK	Mitogen Activated Protein Kinase
MIBC	Muscle Invasive Bladder Cancer
MMP	Matrix Metalloprotease
NAF	Normally Activate Fibroblast
NMIBC	Non-Muscle Invasive Bladder Cancer
PDGFR	Platelet Derived Growth Factor Receptor
PDK1	Phosphoinositide dependent Kinase-1
PI3K	Phosphoinositide 3-Kinase
POSTN	Periostin
ROS	Reactive Oxygen Species
RTK	Receptor Tyrosine Kinase
TGF-b	Tumor Growth Factor-b
TIMP	Tissue Inhibitor of Metalloprotease
TME	Tumor Microenvironment
VEGF	Vascular Endothelial Growth Factor
VIM	Vimentin
TAM	Tumor Associated Macrophage

1. Introduction

Section 1: Bladder Cancer

1.1. Bladder Anatomy and Histology/Physiology

The urinary bladder serves the role of urine storage and exertion from the body. Urine is produced in the kidneys, transported to the bladder through the ureters, and later exerted from the organism through the urethra. Anatomically, the bladder is compartmentalized into four main parts: the apex part, the fundus or base part, the body, and the neck. The body is located centrally with the apex in the anterior front and the fundus in the posterior end. The ureters are directed towards and entering the base of the bladder. The urethra protrudes from the surrounding neck area and is located at the lower part of the organ.[1] Three openings that include the two ureteric and the internal urethral orifices delineate a triangular shape, termed the trigone of the urinary bladder. The detrusor muscle lines the wall of the bladder and contracts to prevent reflux of the content fluids backwards, while physically forming the internal urethra sphincter. *(Figure 1*)[2]

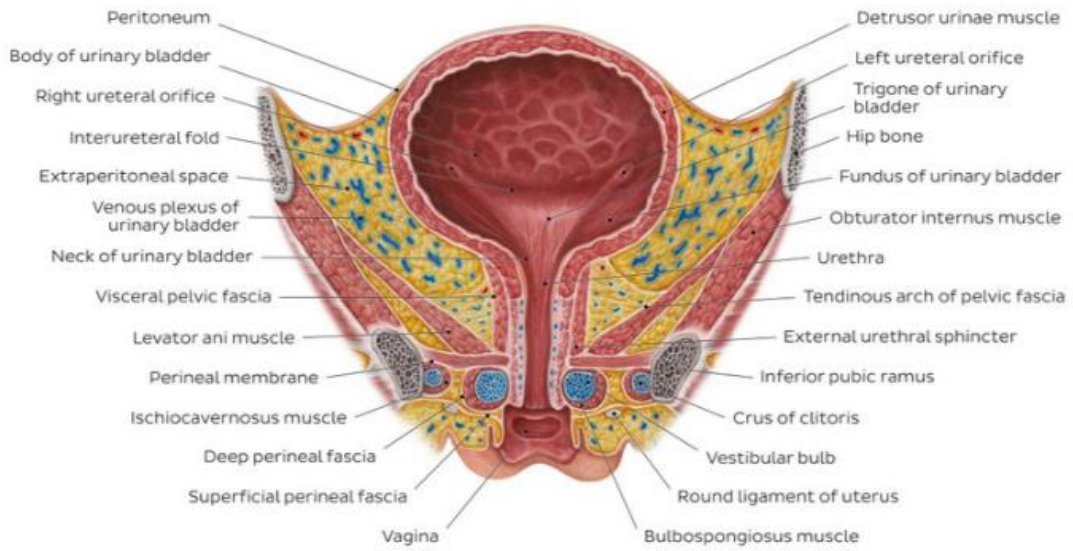

Figure 1: Schematic representation of the female urinary bladder anatomy. https://www.kenhub.com/en/library/anatomy/urinary-bladder-and-urethra

The wall of the bladder comprises four layers, which from the innermost to the outermost are: the mucosa, the submucosa, the detrusor smooth muscle and the serosa or adventitia (*Figure 2*).

- Mucosa: The innermost layer of the bladder, termed the urothelium, is composed of transitional specialized epithelial cells. An epithelial sheet that is in direct contact with the lumen and urine consists of umbrella cells and acts as a barrier between the circulation and urine. Similar to other barriers at epithelial sites, umbrella urothelial cells are located adjacent to a mucus-glycosaminoglycan environment and are connected through tight junctions.

Directed towards the outer part of the bladder, umbrella cells are followed by the intermediate urothelial and basal cell layers that separate them from the submucosa.[1,2]

- Submucosa: The connective tissue layer of the urinary bladder (also known as lamina propria) contains ECM components, including Collagen type I and III, and elastin, as well as fibroblasts responsible for ECM production and remodeling. A vascular and nervous plexus runs the submucosa layer, while resident immune cells elicit immune responses during infections, inflammation and damage. Smooth muscle cells can also be found near innervated areas, surrounding blood capillaries to control vessel contraction. [1-3]
- Detrusor smooth muscle: This part occupies the majority of the tissue, since around 60-70% of the bladder is covered by smooth muscle fibers. Smooth muscle cells in the detrusor are organized in bundles that are maintained conjugated and supported by connective tissue collagens.[14] The detrusor muscle is composed of three consecutive smooth muscle layers, serving the contraction and relaxation functions. The inner and external layer are composed of longitudinal smooth muscle cells, while the middle layer contains circularly localized cells.[1,2,4]
- Adventitia/Serosa: The outermost layer of the bladder. The serosa consists mainly of connective tissue intermingled with adipocytes, known as adventitia, and is lined by squamous epithelium towards the peritoneal part in the upper part of the bladder. [1,2]

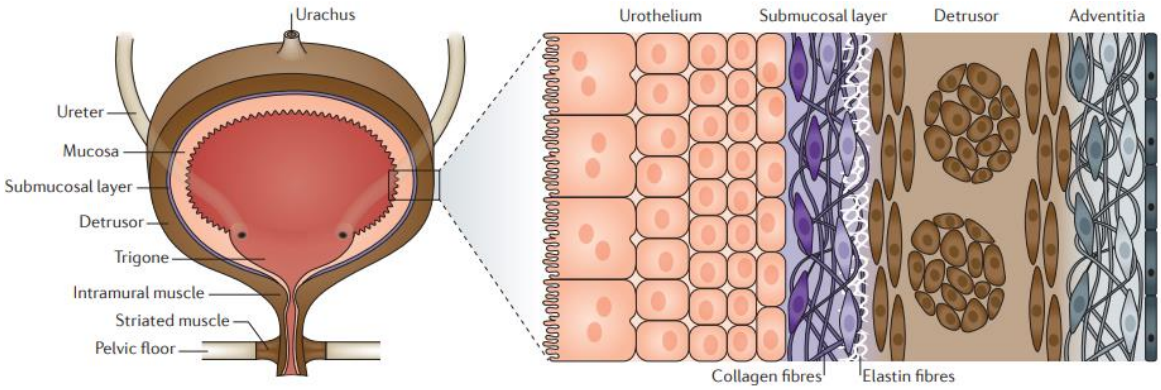

Figure 2: Schematic illustration of bladder wall compartmentalization.
https://www.nature.com/articles/nrurol.2018.5

1.2. Bladder Cancer epidemiology and risk factors

Urinary bladder cancer is classified as the 10th most commonly diagnosed cancer and the 13th in prevalence of cancer-induced mortality, worldwide. It accounts for approximately half million incidences and around 3% of all cancer types annually. It occurs with higher frequency in men, and usually in people over 65 years old. Epidemiologic assessment of bladder cancer geographic distribution reveals that the highest incidence rates are found in Northern America, Southern and Western Europe

(*Figure 3*). United States are the nation with the most dominant occurrence of bladder cancer, hence categorized as the 6th most frequently found neoplasm and the 9th deadliest in the USA.[5,6]

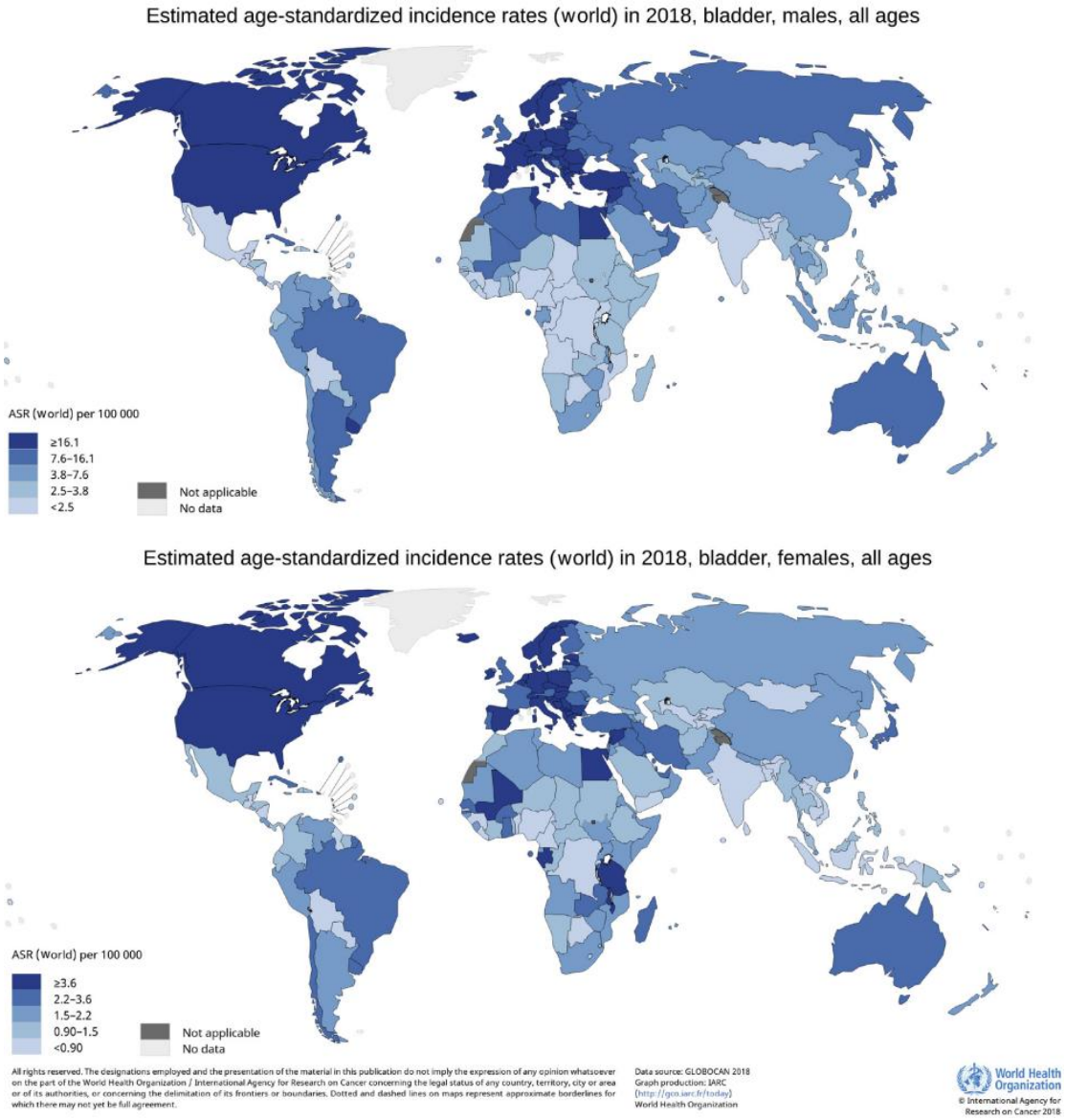

Figure 3: Globocan obtained maps depicting estimated age-standardized incidence rates (ASR) of bladder cancer in 2018, for men and women of all ages. https://doi.org/10.1016/j.eururo.2020.09.006

Hereditary traits are responsible for the familial form of bladder cancer, and environmental factors play a crucial role in predisposition to the disease.[7] Among risk factors for bladder cancer development, tobacco smoking is the most prominent one.[8,9] Smoking, along with hormonal factors and occupational exposure to environmental risk factors also explain the higher prevalence of the disease in men. In addition, tobacco smoking complicates chemotherapy results, worsens survival rates and causes higher relapse incidences in patients undergoing manipulative surgery, such as cystectomy. Chronic urinary tract infection, cancer therapies (cyclophosphamide), radiotherapy, obesity, diet, alcohol consumption and Schistosomiasis also contribute

to the formation of bladder malignancy. Schistosomiasis, which refers to *Schistosoma haematobium* protozoan infection, accounts for the majority of cases in Africa.[10,11]

1.3. Classification and staging of bladder cancer – Histologic variants

Bladder cancer displays heterogeneous manifestations based on histopathologic features. The vast majority is attributed to urothelial bladder cancer, accounting for 90% of cases.[12] As its name implies, the urothelial subtype emerges from the mucosal urothelium alongside the bladder's lumen. Pure urothelial cancer accounts for the majority of cases, but variable differentiation patterns, including squamous, glandular, nested, microcystic, micropapillary, lymphoepithelioma-like, plasmacytoid and sarcomatoid can also be found, a phenotype known as divergent differentiation. [13] Pure urothelial cancer is associated with better prognosis, lower progression rate and lower invasiveness risk than those with divergent differentiation. [14] The squamous differentiation pattern is the second most frequent and is characterized by the existence of keratin conjugates in neighboring epithelial cells. [15] It is commonly reported to occur in combination with the glandular form, which is rarely presented individually. The nested motif appears as nests or cysts in the bladder and is rare, highly aggressive and associated with poor prognostic outcome.[16] The micropapillary type is associated with escalated cancer progression and bad prognosis.[17] Other differentiation patterns represent rare subtypes with little amount of information in the literature. The rest 10% of bladder cancer patient cases corresponds to non-urothelial types, encompassing squamous cell carcinoma, small cell carcinoma, adenocarcinoma, and sarcoma (*Figure 4*).

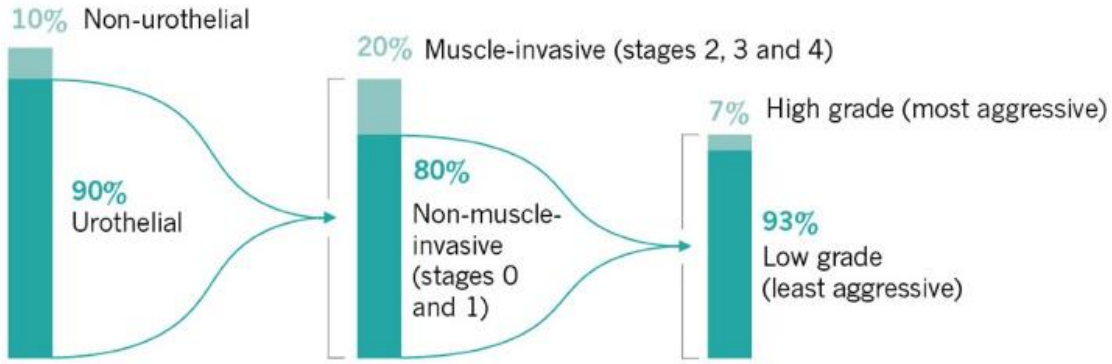

Figure 4: Percentage representation of bladder cancer subtypes, stages, and grades. https://www.nature.com/articles/551S34a

The most commonly diagnosed urothelial cancer type can be sub-classified as muscle and non-muscle invasive, based on the capacity of tumors to spread and invade the detrusor muscle. NMIBC includes malignant transformations belonging to stage 0 or stage 1. Tumors in stage 0 can be either papillary carcinomas (stage Ta) or CIS (stage Tis). CIS is more aggressive and likely to expand in the connective tissue layer beside the urothelium and hence reach stage 1 (T1).[18] MIBC encompasses highly aggressive tumors with metastatic dynamics that have already spread to the muscle layer and

belong to stages 2-4 (T2a, T2b, T3, T4), based on whether they have invaded the lymph nodes and beyond. (*Figure 5*) Newly diagnosed cases of non-muscle invasive bladder cancer range from 70 to 80 %, and from the rest 20 to 30% of muscle-invasive urinary bladder cancer approximately half are metastasizing. [19] (*Figure 4*)

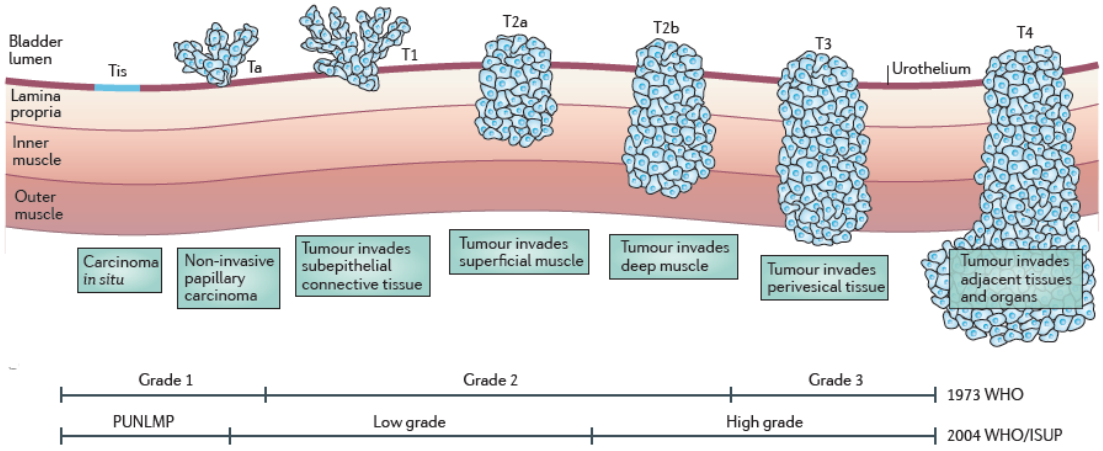

Figure 5: Staging and grading of urothelial bladder cancer based on invasiveness and aggressive behavior. https://www.nature.com/articles/nrc3817

Despite the availability of treatment options in early stages of the disease, recurrence rates reach 60-70% post-operatively for non-muscle invasive bladder cancer. [20] In addition, patients suffering from the muscle-invasive form have worse prognosis, the 5-year survival rate dampens dramatically and therapeutic interventions are more complicated and less effective.[21] Therefore, more sensitive predictive markers are required, along with deeper insight in the molecular mechanisms driving disease pathogenesis, which could enable the design of novel and more effective treatment strategies. Interestingly, immune checkpoint inhibitors have recently provided a promising therapeutic alternative mainly for invasive bladder tumors, highlighting the vital role of cancer cell interactions with surrounding stromal cells in the establishment and progression of the disease.[22]

SECTION 2: CANCER ASSOCIATED FIBROBLASTS

2.1. The Tumor Microenvironment

Tumor development and progression does not depend exclusively on cancer cells. Transformed cancer cells are hosted in a local tissue environment, and are surrounded by heterogeneous cell types and mediators that build a permissive niche for tumor growth, invasion, and metastasis. This dynamic network is termed tumor

microenvironment (TME), and consists of stromal cells and acellular components that form the extracellular matrix (ECM).[23] The stromal cellular component of the TME includes local and infiltrating immune cells, quiescent and activated fibroblasts, pericytes, endothelial cells of capillaries and glial cells. (*Figure 6*) Stromal and cancer cells interact with each other both through physical contact and paracrine signaling. Expression of receptor-ligand pairs, cytokines, chemokines, mitogens, vesicles, and a variety of other signaling molecules allow the establishment of complex communication patterns supporting altered cell phenotype and function.[24]

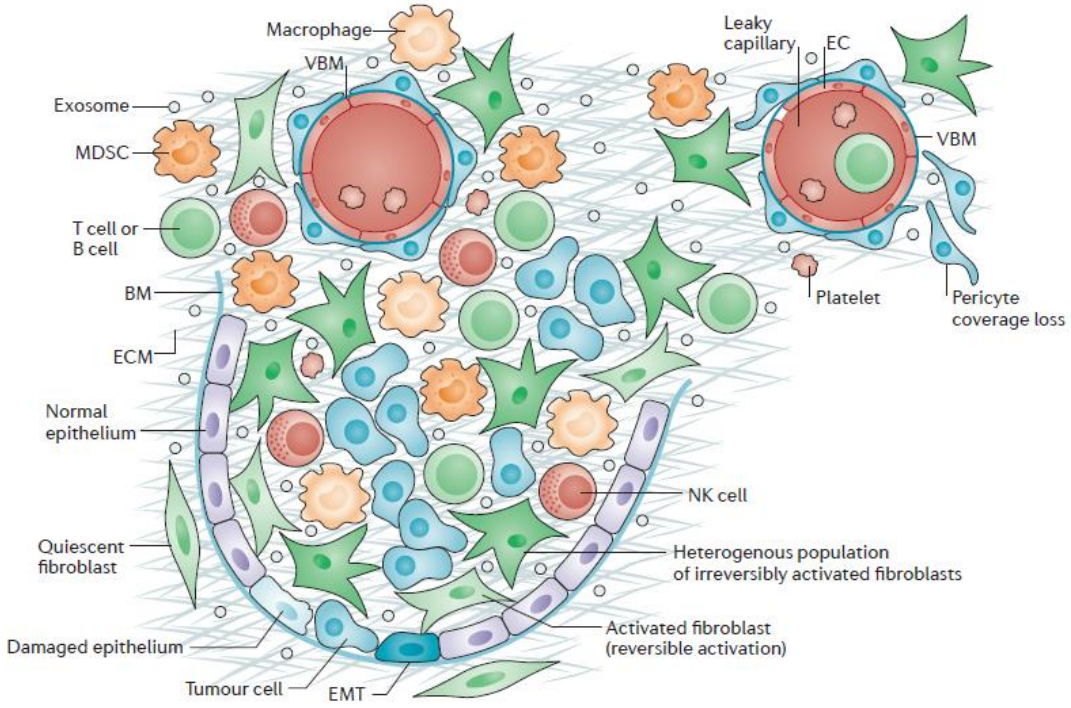

Figure 6: Heterogeneous cell populations of the TME surrounding tumor cells. https://www.nature.com/articles/nrc.2016.73

2.2. Cancer associated Fibroblasts (CAFs) – Activation and origins

Fibroblasts are non-hematopoietic, non-endothelial, non-epithelial cells found as part of the connective tissue within organs.[25] Primarily, they display a supportive role through the production and remodeling of ECM. Through the production of cytokines, chemokines and trophic factors, fibroblasts also perform vital homeostatic functions, including regulation of vascularate functions, immune responses, stem cell maintenance and differentiation.[26] Normal fibroblasts residing within tissues are considered non-proliferative quiescent cells with negligible secretory capacity.[27] Nevertheless, they play an integral role in tissue preservation and normal function under physiological conditions. Activation of fibroblasts has been linked to elevated and robust secretory and metabolic activity, more intense ECM remodeling and increased proliferation.[28] Activated fibroblasts can either return to their previous state or become permanently activated.[29] Reversible activation has been described as a

crucial mechanism during wound healing procedures and resolution of acute inflammatory responses.[30] In contrast, permanent activation, accompanied by genetic and epigenetic alterations of fibroblasts is present in pathologic conditions, including non-resolving inflammation, fibrosis, and cancer (*Figure 7*).[31] In cancer, activated fibroblasts are referred to as cancer-associated fibroblasts (CAFs). Although their role in early stages of tumorigenesis could be considered hindering, current advances in literature mainly support the tumor-promoting role of CAFs.[32]

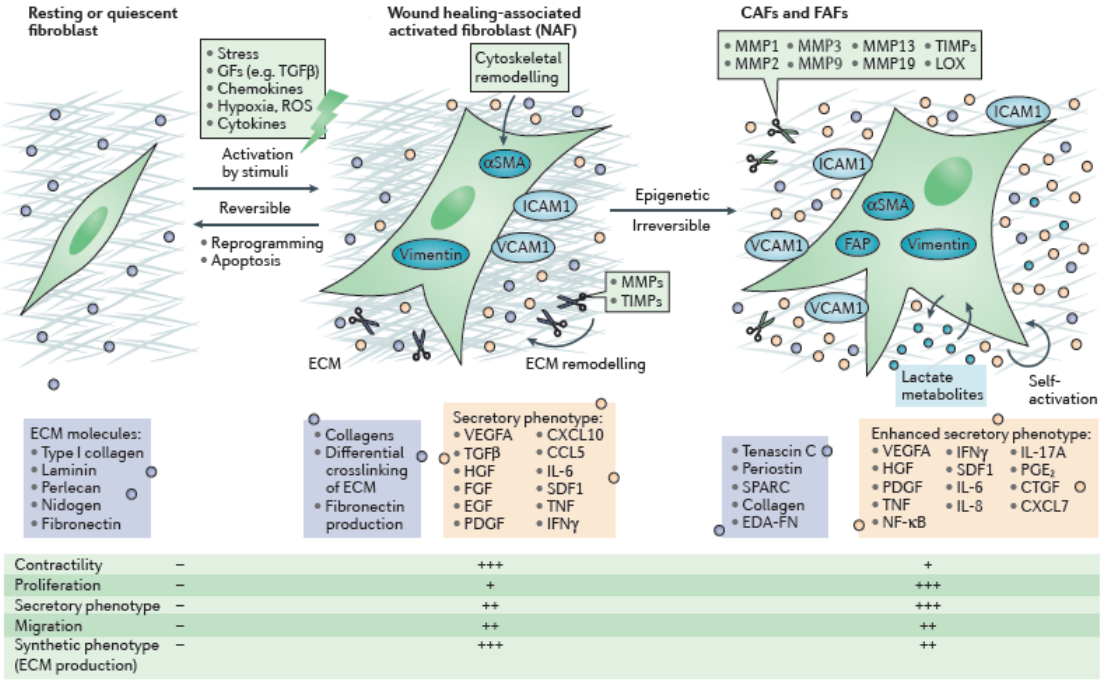

Figure 7: Reversible fate of NAFs and irreversible pathogenic activation of CAFs and FAFs. https://www.nature.com/articles/nrc.2016.73

Due to lack of selective molecular markers, specific identification of CAFs has been challenging. As such, CAFs are defined by a combination of features, including increased deposition of collagen, fibrin and ECM molecules, lack of endothelial, immune, and epithelial cell marker expression and positive labelling for markers associated with fibroblast activation, such as a-SMA and FAP.[33] Apart from CAF identification, the absence of specific biomarkers complicates lineage-tracing and fate-mapping experiments and as such the tracing of CAFs origins. Nevertheless, resident tissue fibroblasts represent the main source of CAFs.[34] CAFs have also been reported to originate from bone marrow-derived mesenchymal stem cells through a TGF-b1/JAK/STAT3 signaling axis[35], endothelial cells through EndoMT [36], and epithelial cells via EMT. Additional potential cellular sources include stellate cells present in the liver and pancreas, pericytes, smooth muscle cells, adipocytes, hematopoietic- and cancer- stem cells (*Figure 8*).[37]

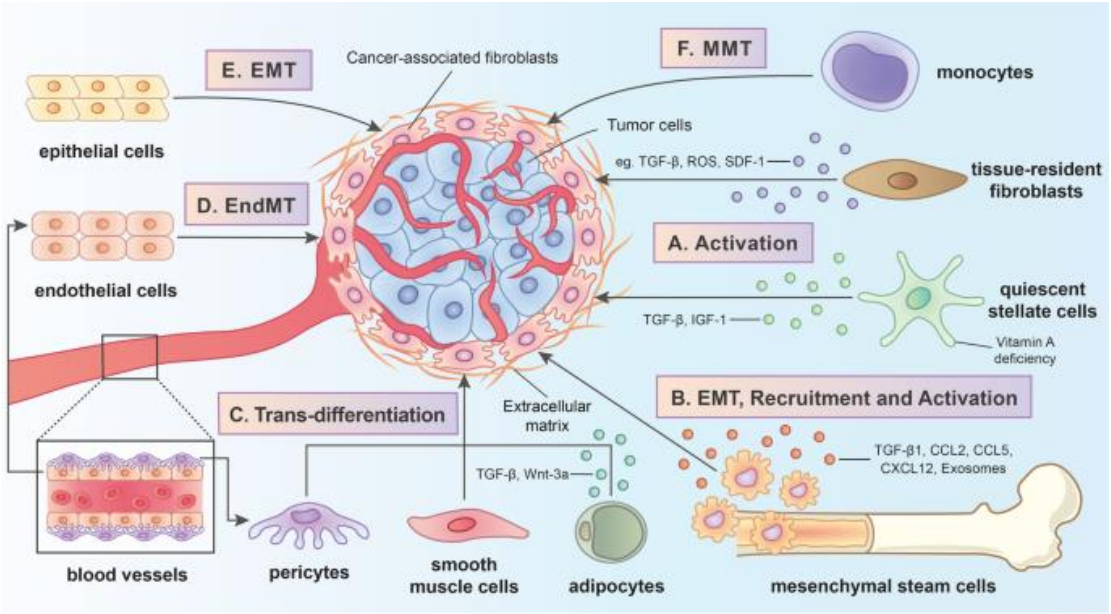

Figure 8: The origins of CAFs. https://molecular-cancer.biomedcentral.com/articles/10.1186/s12943-021-01428-1

The vast majority of activating signals derive from transformed tumor cells through cell-to-cell contact (e.g. Notch signaling) and secreted soluble mediators. Growth factors (PDGF, HGF, FGF, TGFβ), HSF-1, ROS, hypoxia, stress, pro-inflammatory cytokines (IL1, IL6), chemokines (CXCL12, CXCL16, CCL21, CCL25), double strand breaks and DAMPs, as well as metabolites like lysophosphatidic acid induce the activation of fibroblasts to CAFs.[26,31,38] Downstream pathways include activated NFkB, JAK-STAT and SMAD pathways. [39-41]Specifically in bladder cancer, tumor cells have been found to release exosomes transferring TGF-b in order to trigger SMAD signaling pathways and mediate activation of tissue-resident fibroblasts into CAFs.[42] In addition, increased stiffness and mechanical forces applied by the ECM represent another important regulator of CAF activation.[43] Finally, therapeutic interventions, such as radiotherapy, chemotherapy and targeted compounds are known to affect fibroblast fate and function. [44,45]

2.3. CAF functions in tumor initiation, progression, and metastasis

CAFs exert pleiotropic functions, including both pro- and anti-tumorigenic ones, and affect all the pathogenic properties of malignant cells. For the purpose of the current thesis, the role of tumor-promoting CAFs will be further described, since it is the most well-established. Owing to the elevated secretory capacity of CAFs, a repertoire of growth factors, cytokines, chemokines, metabolites, enzymes, ECM constituents and remodeling factors establish the development of cancer hallmarks.[46] Therefore, CAF secretome enhances tumor cell proliferation, self-renewal and survival, angiogenesis, immune suppression, metabolic alterations and ECM remodeling that mediate cancer progression, invasion and metastasis (*Figure 9*).[47]

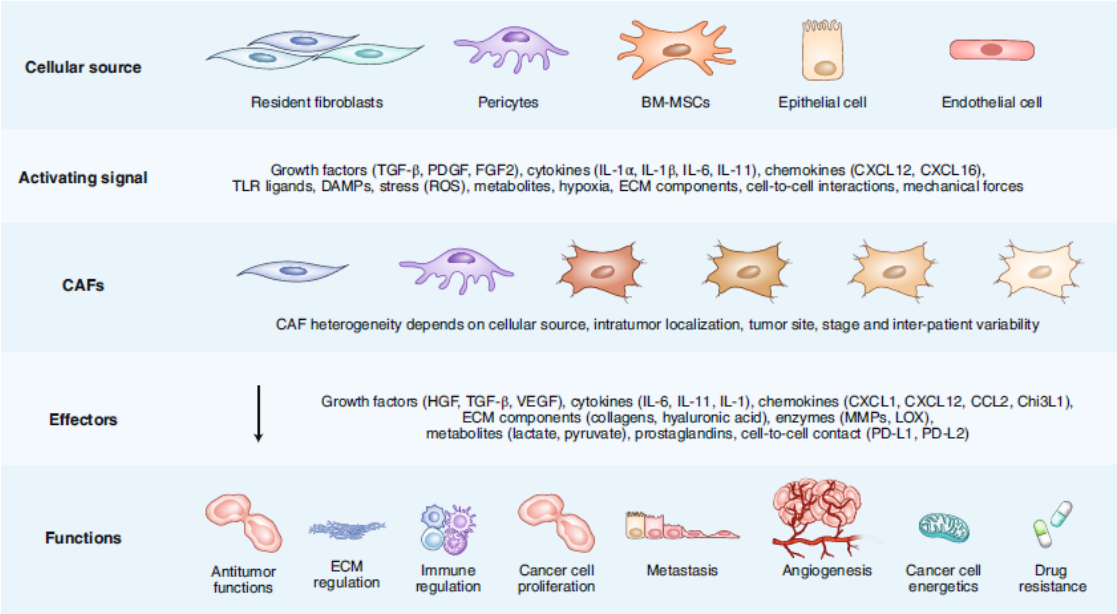

Figure 9: Origins and functions of CAFs in cancer. https://www.nature.com/articles/s41590-020-0741-2

ECM remodeling

CAFs in the tumor stroma primarily serve the role of ECM deposition and remodeling to create a permissive niche for enhanced cancer cell motility and invasion (*Figure 10*).[48] This is accomplished mainly through the dynamic production of ECM components and secretion of proteolytic enzymes, including MMPs and TIMPs.[49] For instance, MMP3 cleaves molecules involved in cell-to-cell contact, such as E-cadherin leading to increased cancer cell motility.[50] TIMPs as inhibitors of MMPs are negatively associated with cancer cell migration. For example, TIMP deficiency in fibroblasts induces the release of exosomes enriched in MMPs, ADAM10 and disintegrin leading in altered ECM composition enabling invasion and cancer stemness.[51] CAFs promote metastasis through the maintenance of cancer stem cells in secondary sites and by secreting enzymes that mediate ECM crosslinking creating a stiff microenvironment with tense mechanical forces.[52] Increased mechanical conductivity is related to severe manifestations of the disease, including stress induction, hypoxia, aggressiveness and drug resistance.[53] For example, formation of integrin-related adhesions in the ECM and the cytoskeletal actin-myosin system are regulated by CAFs through RHO, RAB-GTPase, and YAP activity.[54,55] Tenascin-C and POSTN are two examples of molecules produced by CAFs to provide WNT signals in appropriate stem cell niches, like the one acting in colorectal cancer.[56,57]

Cancer cell proliferation, invasion and metastasis

CAFs secrete a variety of paracrine signals to interact with neighboring cancer cells. HSF-1 activated in CAFs creates a tumor-permissive stroma and reprograms malignant cells for the initial establishment of tumor formation.[58] Several growth factors, including HGF, FGF5, GDF15, GAS-6, LIF and predominantly TGFβ produced by CAFs are vital drivers of tumor expansion, survival, invasive behavior and colonization in

metastatic locations.[31] TGFβ is a master regulator of EMT and as such a major contributor to cancer metastasis. For instance, TGFβ1 upregulates HOTAIR to induce EMT, resulting in breast cancer metastasis.[59] In addition, CAFs themselves employ TGFβ signaling in an autocrine manner to preserve their activity status through a TGFβ1/miR-200s/miR-221/ DNMT3B dependent mechanism. [60]

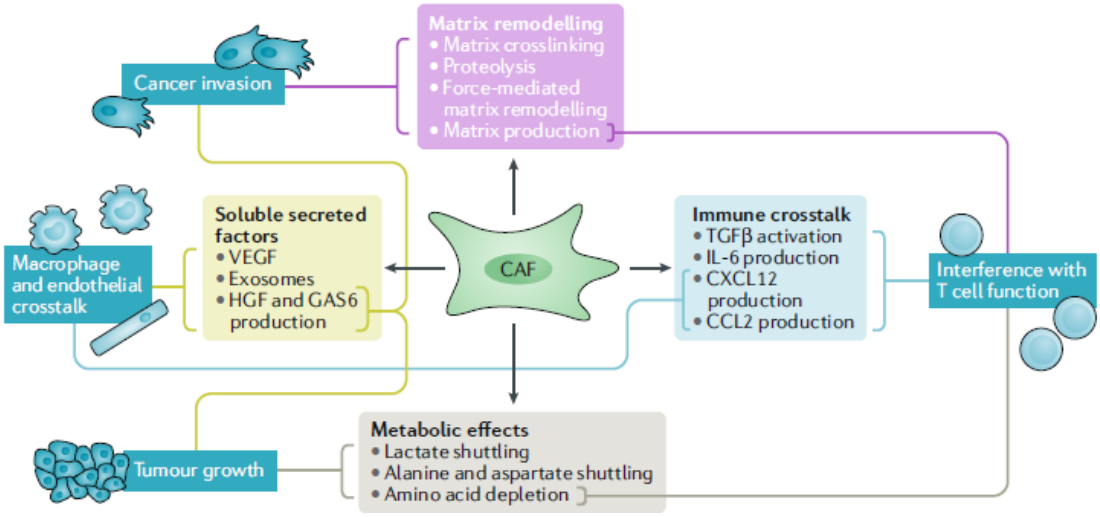

Figure 10: CAF functions in mediating tumor growth, invasion and metastasis. https://www.nature.com/articles/s41568-019-0238-1

Some of the above factors have been also associated with resistance to treatments, like HGF that confers resistance to BRAF-related therapies.[61] Cytokines, including IL-6, IL-1 and IL-11 also have tumor promoting functions. For example, IL-6 increases cancer cell proliferation, motility and resistance to treatments through activation of the JAK2/STAT3 pathway.[62] CAF-derived IL11 promotes viability of cancer stem cells in colorectal cancer.[63] Other signals, like STC1 favor metastasis through enabling tumor cells to transport through the endothelium wall of capillaries.[64] Tumor expansion is also fueled by CAFs through the production of factor that support increased angiogenesis, including SDF-1 (CXCL12) and VEGF.[65]

Metabolic reprograming

CAFs exhibit shifts in their metabolic activity. Several metabolites and factors are transmitted bi-directionally between cancer cells and CAFs serving the demanding functions of both cell populations (*Figure 11*).[66] Cancer cells stimulate aerobic glycolysis in CAFs, through establishment of hypoxia, release of PDGF, TGFβ, HIF1α and ROS-mediated downregulation of CAV1.[67-69] In turn, CAFs produce metabolites, such as lactate, ketone bodies and fatty acids to nourish anabolic mitochondrial respiration in cancer cells.[70] As such, tumors have the capacity to growth, invade neighboring spaces and resist damaging insults. This phenomenon is known as the "Reverse Warburg effect".[71] This mutual exchange of factors also elevates catabolic activities and autophagy in CAFs. Autophagy can drive the production of alanine from activated fibroblasts, which is transferred to pancreatic cancer cells in order to fulfill their metabolic demands.[72] Apart from tumor cells, metabolites and amino acids

derived from CAFs can also affect immune cellular properties and function.[73] For example, upregulation of IDO1 and ARG in CAFs leads to decreased tryptophan and arginine, respectively, and negatively affects the activation, proliferation and normal effector function of T cells, contributing thus to immunosuppression.[74,75]

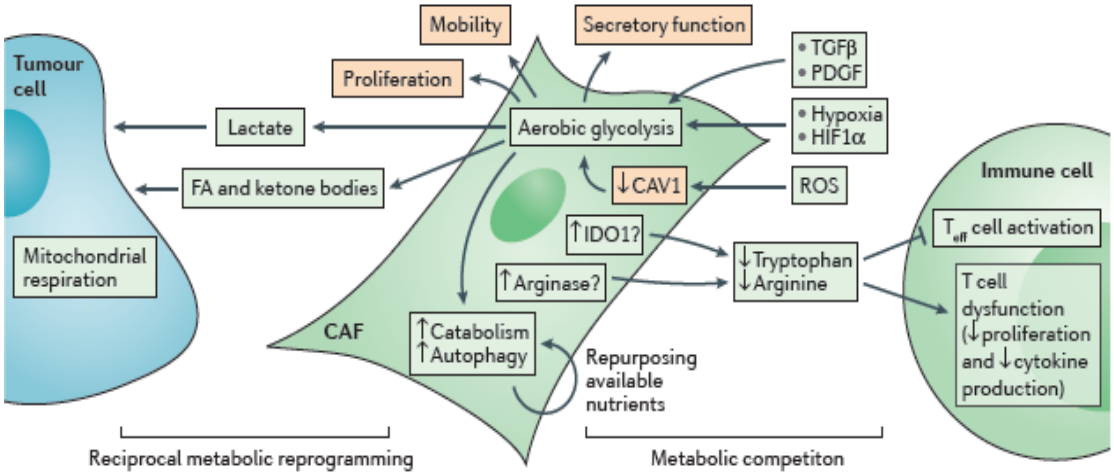

Figure 11: The metabolically reprogrammed landscape of tumors centered on CAF activity. https://www.nature.com/articles/nrc.2016.73

Immune regulation

CAFs are engaged in a highly dynamic and complex communication network with neighboring immune cells, and exert pleiotropic effects on tumor immunity. The majority of studies support an immunosuppressive role of CAFs that is achieved through the secretion of cytokine and chemokines (*Figure 12*). Induction of M2 macrophage polarization, differentiation and recruitment of immunosuppressive cells and altered T helper cell differentiation towards Th2 type of responses, result in cancer cells evading immune surveillance.[76,77] IL-4, IL-6, IL-8 and TGF-β are the major contributors in the creation of immunosuppressive environment facilitating cancer escape.[78]IL-6 mediates its effects mostly through STAT3 signaling and downstream activation of IFN-γ and IL-17A. [79,80] TGF-β affects T_H17 cell differentiation and inhibits the cytotoxic activity of effector T cells.[81] Suppression of effector T cell activation and cytotoxic function have also been attributed to CAFs expressing co-inhibitory signals including PD-L1 and PD-L2.[82,83] CAFs alter immune cell trafficking and recruitment to the affected tissue, through expanding the capillary network, providing adhesion molecules, such as ICAM1, remodeling the ECM and expressing chemokines, including CCL2/ 5/ 7/ 8 and CXCL1/ 2/ 5/ 9/ 10. [29,84]

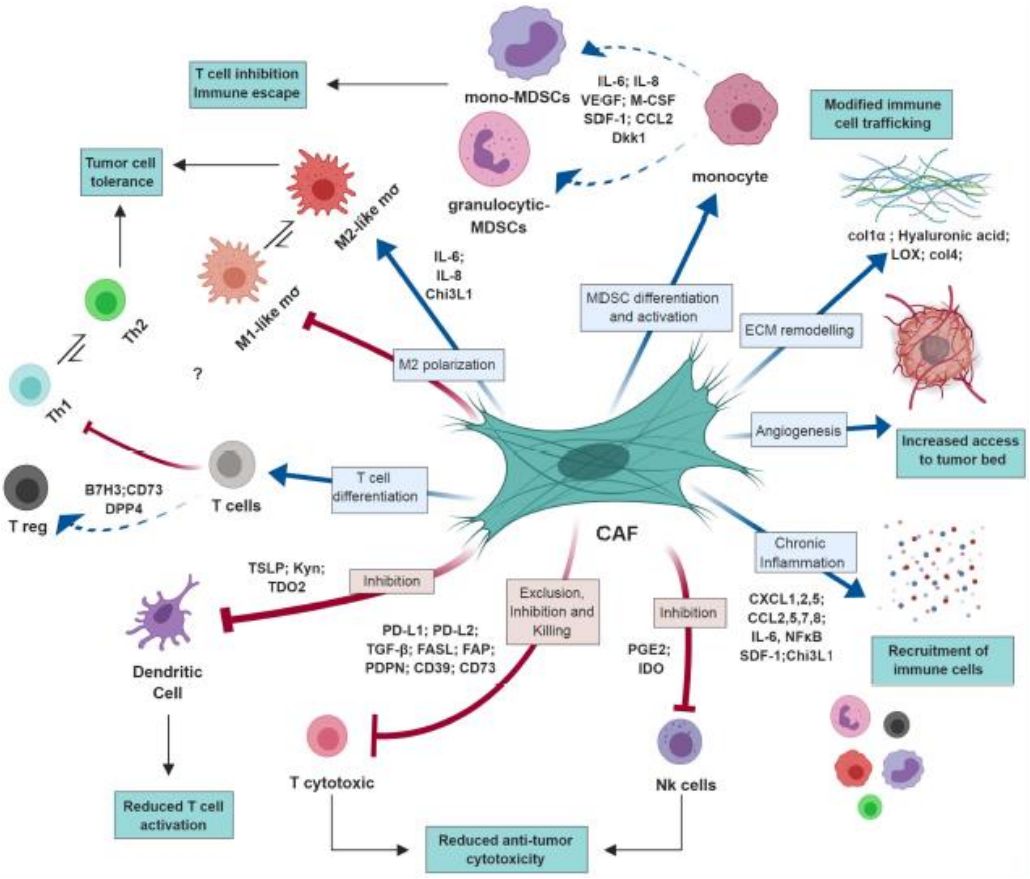

Figure 12: Orchestration of CAF immunosuppressive function.
https://www.frontiersin.org/articles/10.3389/fimmu.2019.01835/full

2.4. CAFs in bladder cancer

Although recent advances have enhanced our understanding of CAF-driven mechanisms in carcinogenesis, little information exist regarding their role specifically in urothelial bladder cancer. CAFs in urothelial bladder cancer have been reported to express a-SMA, FAP, MFAP5, vimentin, PDGFR-a/b, CD90 and FSP1. [85] Among them, a-SMA, CD90/Thy-1, FAP, PDGFRa and PDGFRb have been correlated with decreased survival rates of patients suffering both from MIBC and NMIBC. FAP expression is linked to the poorest 5-year survival probability, while CD90 is associated with comparatively elevated CD8a T cell infiltration.[86] CAF-specific MFAP5 has been shown to promote the tumorigenic potential of bladder cancer cells through NOTCH2/HEY1 signaling, while being associated with poor clinical outcome.[87] CALD1 expression in urinary bladder cancer CAFs enhances tumor progression and is proposed as a prognostic marker.[88] TGFβ signaling in CAFs is associated with impaired infiltration of CD8+ T cells in urothelial cancer and resistance to anti-PD-L1 immunotherapy.[132] In addition, urinary bladder cancer CAFs secrete TGFβ1 and IL6, which promote EMT, enabling thus tumor expansion and invasion.[89-91] Finally, CAFs have been found to promote cisplatin resistance in patients, by enhancing IGF-1/ERβ/Bcl-2 anti-apoptotic signaling in bladder tumor cells. [92]

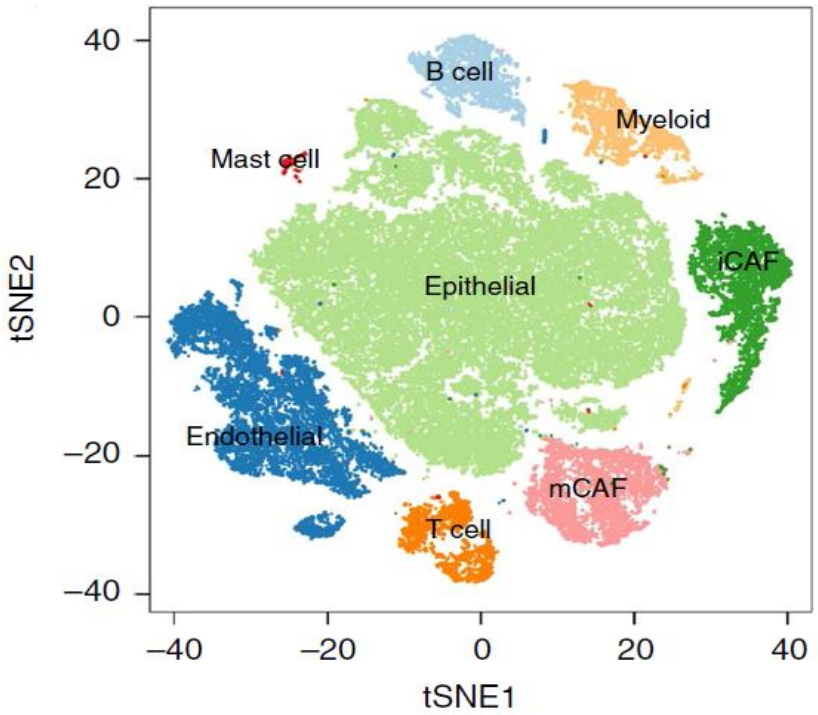

Figure 13: Plot depicting single cell RNA sequencing-derived cell subpopulations present in urinary bladder cancer patients. https://www.nature.com/articles/s41467-020-18916-5

Interestingly, a recent single-cell transcriptomic analysis identified two distinct Col1a1^{+} CAF populations in urothelial bladder cancer, termed inflammatory-CAFs (PDGFRa^{+} iCAFs) and myo-CAFs (RGS5^{+} mCAFs), in line with similar studies in other cancers (*Figure 13*).[93] Transcription analysis revealed activation of TCF21 and TWIST2 in iCAFs, affecting smooth muscle behavior and EMT in other pathologies, like breast cancer and atherosclerosis respectively.[94,95] iCAFs secrete high levels of CXCL12 to drive recruitment of TAMs through signaling to its CXCR4 receptor.[96] Angiogenesis could be influenced accordingly through production of VEGFA and VEGFB. FGFR1, FGF2 and FGF7 expressed by iCAFs could participate in autocrine signaling forming a positive feedback mechanism of fibroblast activation.[97] Among the growth factors secreted by iCAFs, IGF-1 is of particular interest as it is specific for iCAFs and associated with poor survival rates.[93]

SECTION 3: IGF1 SIGNALING AND FUNCTION

3.1. IGF1 and downstream signaling pathways

IGFs are known mitogens driving growth-promoting processes. The most studied members are IGF-1 and IGF-2 that mediate biological effects through signaling to Insulin-like growth factor receptors IGF-1R and IGF-2R, respectively.[98] IGFRs belong to the family of RTKs. Normally, signal transduction to IGF-1R is essential to regulate cellular events, while IGF-2R lacks functional kinase activity and targets IGF2 towards

lysosomal degradation.[99] IGF receptors exist as dimers consisting of two extracellular α chains that bind to the ligand and two transmembrane β chains that exhibit tyrosine kinase activity. [100] IGF-1 bears higher binding affinity for IGF-1R/1R homodimers. Due to its high homology with Insulin, IGf-1 also has the capacity to bind to IR homodimers and IGF-1R/IR heterodimers, although with lower affinity.[101] IGFs mainly exist in conjugates with IGFBPs that control ligand availability to the receptors. There are six members of IGFBPs with differential expression in blood circulation and peripheral tissues and binding affinity for IGF1.[102] The majority of IGF1 molecules, around 75% are bound to IGFBP3 and ALS.[103] IGFBPs remain bound to the growth factors to increase the half-time of their life and hinder signaling to the receptors when not demanded. Once IGF-1 is released from the IGFBP and binds to its receptor, it triggers conformational alterations that lead to the expansion of the activation loop and enable stimulation of the kinase activity.[104] As a result, transphosphorylation events take place in the tyrosine residues Y1135, Y1131, and Y1136 of the intracellular terminal domains.[105] Following the conformational changes and tyrosine phosphorylation, specific substrate proteins are recruited to the phosphorylated tyrosine residues through SH2-domain mediated interactions. Shc and IRS-1/IRS-2 are the best-known substrates that lead to coupling of the initial axis stimulation with second messenger systems and downstream signaling cascades.[106] Phosphorylation of IRS-1 and IRS-2 by the kinase activity of the receptor trigger the PI3K-PDK1-Akt signaling pathway, while phosphorylation of Shc leads to activation of the MAPK signaling cascade (*Figure 14*). Phosphorylated IRS-1 / IRS-2 and Shc interact with the adaptor proteins Grb2 and p85 regulatory subunit of PI3K through SH2 domain recognition, respectively.[107] Downstream, Grb2 recruits a guanine nucleotide exchange factor, termed SOS. SOS controls the exchange of GTP/GDP to RAS GTPase, engaged either in RAS-GTP active form or RAS-GDP inactive state.[108] RAS triggers the RAF-MEK-ERK cascade of sequential activating phosphorylations. MAPK signaling results in the initiation of transcriptional programs in the nucleus that promote cell proliferation and survival.[109] The second pro-survival pathway is triggered by PI3K recruitment to IGF1R. The catalytic subunit of PI3K, termed p110a controls conversion of PIP2 to PIP3 that facilitates recruitment of PDK1.[110] PDK1-mediated phosphorylation at Threonine residue, T308 and mTORC2-mediated phosphorylation at Serine residue, S473 of Akt enable the complete activation of the serine/threonine kinase. [111] Akt phosphorylates a variety of molecular targets, including TSC1/2, GSK-3β, p27, FOXOs, BAD and BCL-2 to regulate cell proliferation, survival, apoptosis and glucose metabolism.[112]

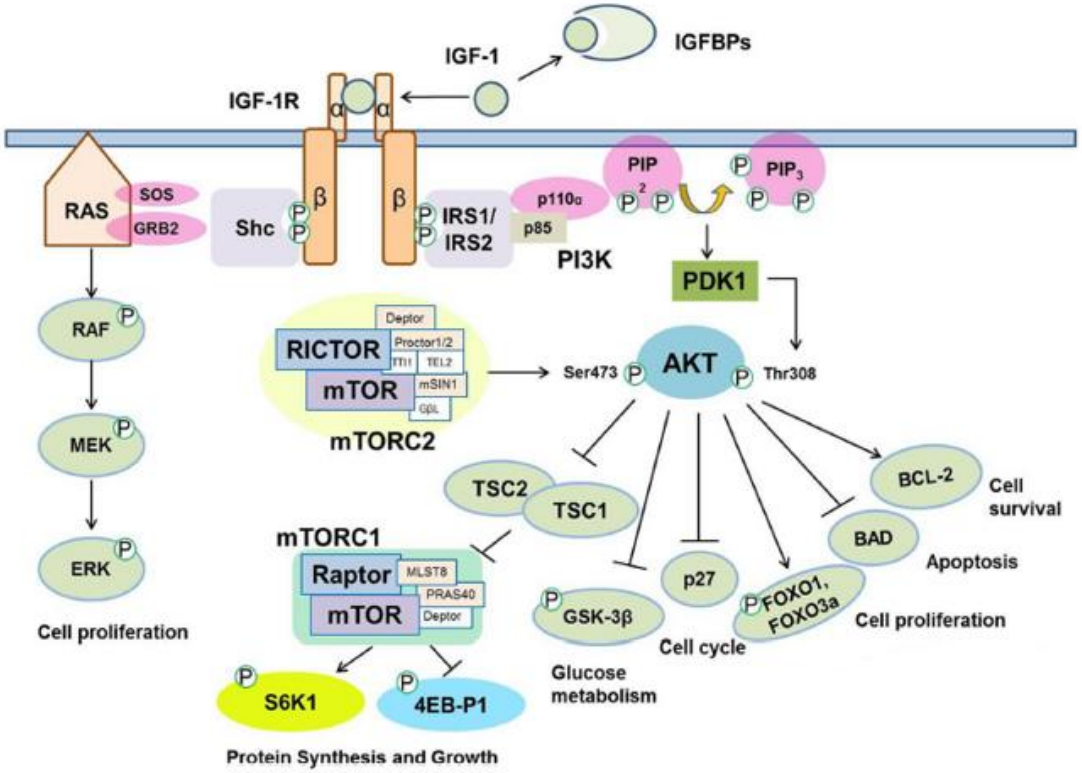

Figure 14: Schematic representation of IGF-1 signal transduction pathways. https://www.ncbi.nlm.nih.gov/pmc/articles/PMC4292735/

3.2. IGF1 in homeostasis-physiology

The pleiotropic physiological actions of IGF1 in human organism have been initially attributed to the 'somatomedin hypothesis'.[113] Based on this hypothesis, IGF1 mediates the growth-promoting effects of growth hormone (GH) upon biological systems. GH is released in systemic blood circulation from the pituitary in response to GHrH from the hypothalamus (*Figure 15*).[114] GH induces the synthesis of 'somatomedins', meaning IGFs in the liver. IGF1 is predominantly produced by the liver and secreted in the circulation to function as an endocrine factor through signaling in peripheral organs.[115] The GH – IGF1 axis is regulated by a negative feedback loop, where IGF1 reaches the hypothalamus through blood circulation and promotes the release of somatostatin, a negative regulator of GH and GHrH secretion (*Figure 15*).[116] Ghrelin represents an intestinal-derived factor that along with pancreas - derived insulin and adipocyte - derived leptin are also implicated in somatotropic axis control, as a positive regulator of GH release from the brain.[117] The somatomedin hypothesis has been revised, since in vivo studies revealed that liver-specific ablation of IGF1 expression resulted in 75% decrease of IGF1 serum levels, meaning that the rest 25% originates from alternative sources.[118] In addition, *Igf1* knockout mice exhibit growth -developmental retardation and severe loss of body weight in comparison to control, while mice with liver-specific deletion of *Igf1* present normal growth and slight developmental alterations. Recent findings indicate that local production of

IGF1 plays an important role in skeletal growth.[119] In addition, local synthesis of IGF1 has been reported for several other peripheral tissues, including the brain, heart, bone marrow, lung, proximal and distal gastrointestinal tract, urinary bladder, adipose and gender tissues.[120] As such, apart from systemically released IGF1 acting as endocrine factor, IGF1 is also locally produced to function in an autocrine and paracrine manner.

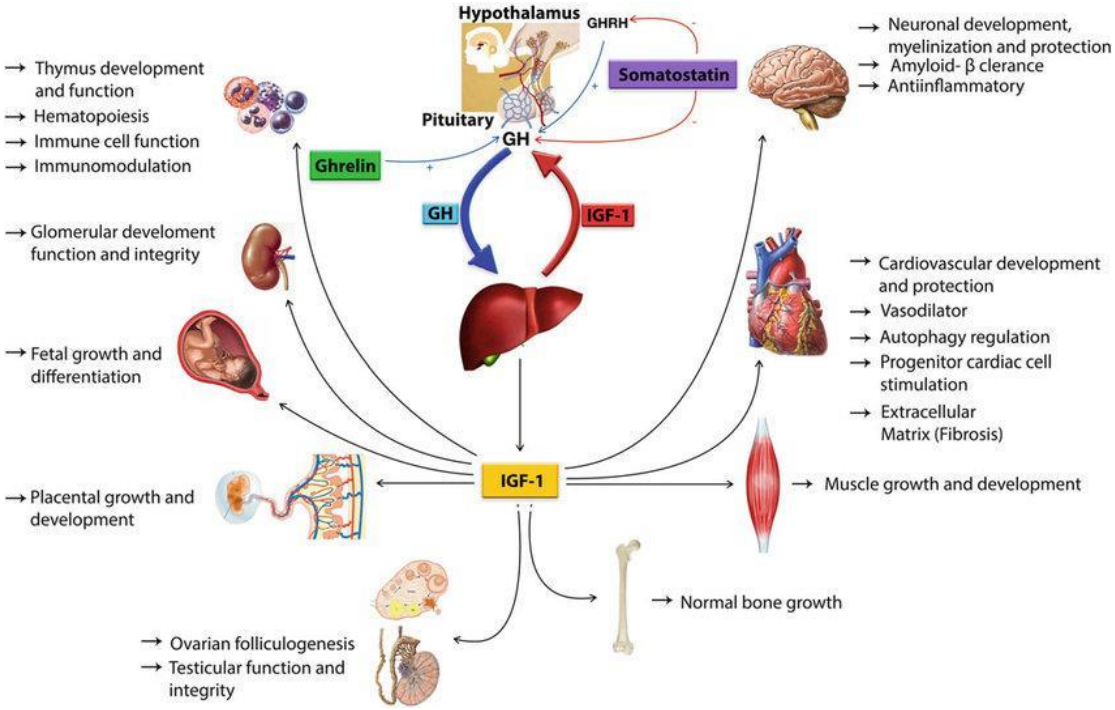

***Figure 15**:* IGF1 production and physiological role in peripheral organs https://link.springer.com/chapter/10.1007/112_2017_8

During prenatal and embryonic stages, IGF1 released under GH control is important for placenta formation and growth, as well as for normal development and differentiation of fetal tissues.[121] In adult life, IGF1 mediates a variety of functions during embryonic and post-natal development, including the stimulation of cellular proliferation, growth, differentiation and survival, exertion of anti-oxidant and mitochondrial protective effects, regulation of lipid, carbohydrate metabolism and insulin resistance (*Figure 15*).[122-125] For instance, IGF1 is responsible for regulating bone length, healthy formation and remodeling through signaling to chondrocytes in the growth plate of appendicular bones and osteocytes, osteoclasts, osteoblasts in radial skeleton.[126] Also, to facilitate skeletal muscle growth and development, IGF1 mediates fusion of myoblasts with myotubes. It has been found to regulate calcineurin levels to control skeletal muscle mass through promoting hypertrophy or attenuating atrophy.[127] Regarding the cardiovascular system, IGF1 exerts protective and growth promotive actions through regulating autophagy, proliferation and commitment of cardiac progenitor cells and promoting vasodilation.[128] Next, IGF1 possesses immune-modulatory roles through stimulating thymus development and hematopoiesis, while coordinating the normal growth and function of immune cells.[129] As growth factor it is also important for the accurate formation and development of kidneys and the reproductive organs in both sexes.[130,131] Furthermore, IGF1 promotes tissue-

protective, reparative and regenerative processes following injury, which has been extensively reported in the liver, central nervous system and heart damage. [132,133]For example, in the central nervous system, IGF1 promotes the proliferation of progenitor cells, neurogenesis, oligodendrogenesis and angiogenesis, while exerting neuroprotective and anti-inflammatory effects following CNS injury.[134] Nevertheless, there are not extensive information regarding the role of IGF1 in bladder homeostasis and physiology besides the well characterized growth promoting effects similar to other organs.

3.3. IGF1 in cancer

Aberrantly elevated levels of the IGF ligands, or overexpression and constitutive activation of IGF-Rs drive pathologic conditions, including cancer. IGF1 contributes to the acquisition of infinite proliferation capacity in cancer through signaling to the aforementioned receptors.[135] IGF-Rs mediate the oncogenic effects of growth factors, driving malignant cell transformation.[136]

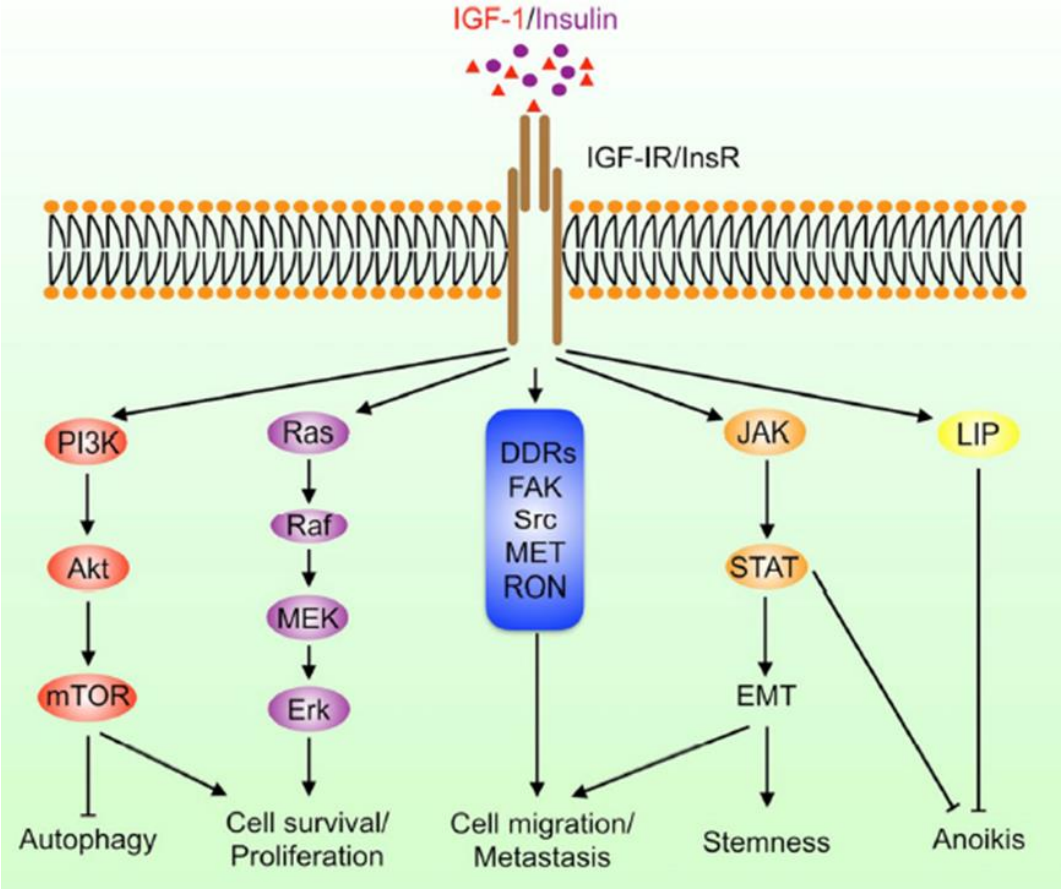

Figure 16: IGF-1 mediated signaling pathways in cancer. https://jhoonline.biomedcentral.com/articles/10.1186/s13045-020-00904-3

Hence, IG1/IGF-1R axis hyperactivation in cancer contributes to the maintenance and migration of cancer and stromal cells, hence promoting tumor development and

metastasis.[137] The major tumor-promoting pathways are MAPK, PI3K and STAT3, positively affecting cellular proliferation and survival, while inhibiting cell death.[138] Also, IGF1 signaling to IGF1R promotes the acquisition of cancer cell stemness and EMT, a known mechanism implicated in carcinogenesis.[139] For instance, activated Akt stabilizes Slug transcription factor that suppresses E-cadherin expression leading to EMT.[140] In addition, IGF1R overexpressed in colorectal cancer stem cells leads to STAT3 activation and expression of transcription factors, such as Nanog that promote both EMT and stemness.[141] Furthermore, IGF1R-induced Akt activation can lead to LIP expression, a factor that suppresses anoikis, a type of cancer cell death (*Figure 16*).[142]

Several studies have explored the prognostic and therapeutic potential of circulating IGF1 levels. Elevated IGF1 in the bloodstream is positively associated with increased risk in many types of cancer, including breast, prostate and advanced colon cancer. [143] In bladder cancer, IGF1 has been reported to possess poor prognostic value as a marker.[144] A major challenge is that IGF1-IGF1R signaling induces resistance to general therapeutic strategies against cancer, including chemotherapy, radiotherapy, endocrine therapy and molecular targeted therapies. [145]

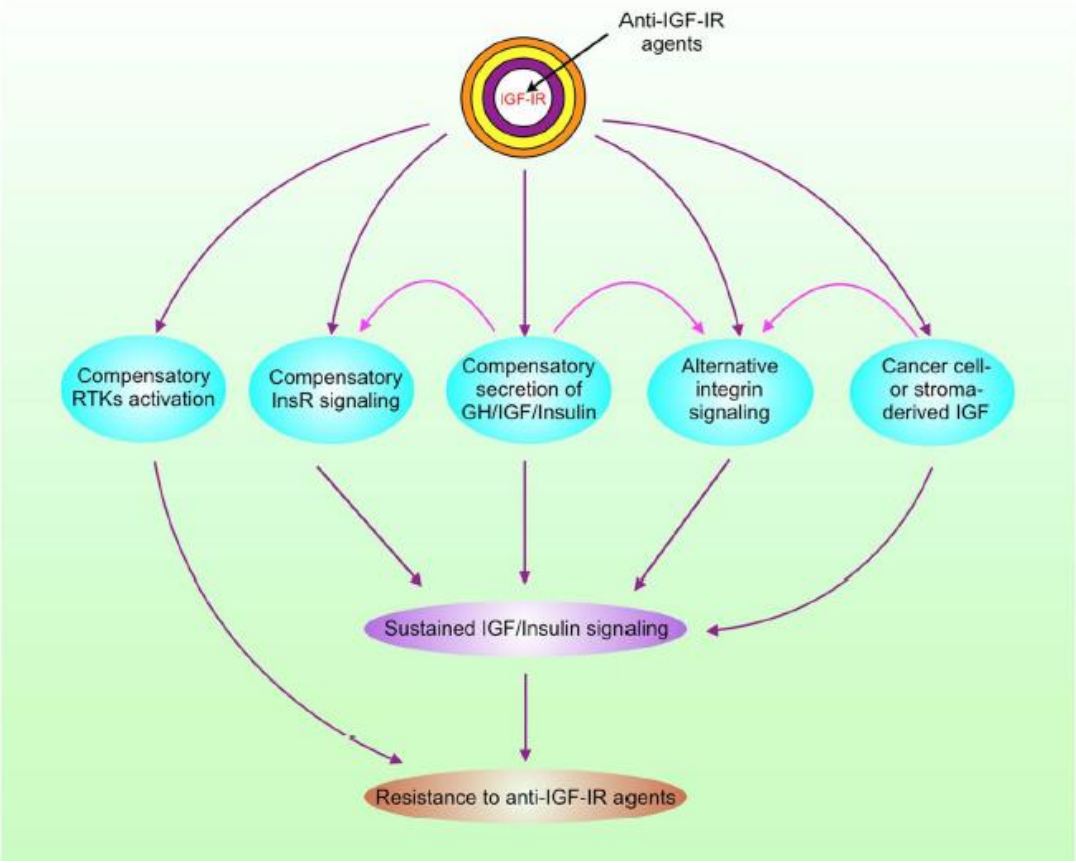

Figure 17: Mechanisms of resistance to therapies targeting IGF1R. https://jhoonline.biomedcentral.com/articles/10.1186/s13045-020-00904-3

Nevertheless, a variety of therapeutic strategies have been designed to target the IGF-1/IGF-1R axis. A second challenge that needs overcoming is the acquired resistance in specific drugs, such as monoclonal antibodies and small molecule inhibitors aimed to

inhibit the oncogenic IGF1 signaling, mainly through targeting IGF1R.[146] Several mechanisms leading to ineffective management of IGF1/IGF1R signaling have been described (*Figure 17*):

● **Compensatory release of Growth hormone, Insulin and IGFs:** Since IGF1/IGF1R signaling axis is implicated in feedback inhibition of growth hormone release, blockage of IGF1R may result in increased secretion of GH and GH-mediated release of IGFs and Insulin.[147] In this case, IR replaces IGF1R in signal transduction from IGFs and Insulin and sustains the tumorigenic potential. This mechanism has been described to apply in breast and pancreatic neuroendocrine cancer, while it has been reported to provide resistance to cixutumumab in preclinical evaluation. [148]

● **Binding to integrin receptors:** IGFs have the capacity to bind and signal to integrin receptors when IGF1R is occupied. Integrin stimulation facilitates cancer cell survival and stemness to cope with therapy-related environmental stress.[149] IGF1 binding to integrin αvβ3 activates PI3K and induces resistance to cixutumumab. [150]

● **Signaling to alternative receptor tyrosine kinases:** Once IGF1R is blocked by targeting inhibitors, other RTK members may get activated to compensate for the signaling loss. Alternative RTKs are also coupled with IRS1, PI3K, MAPK, STAT3 and result in relevant signaling pathways and cellular alterations, as the ones triggered when IGF1R is activated.[146] For instance, EGFR and PDFGRα/β activation is implicated in acquiring resistance to anti-IGF1/IGF1R therapies.[151,152] This mechanism has been described to confer resistance in cases of childhood sarcoma and for specific inhibitory molecules, including dalotuzumab and linsitinib.[153]

● **Contribution of tumor stroma:** Stromal cell populations residing in the microenvironment surround cancer cells can act as a source of IGFs. For example, fibroblasts secrete IGF signaling to IGF1R on malignantly transformed cells, leading in acquired resistance to chemotherapy and radiotherapy.[44,154] Given that IGFs exploit additional receptors and pathways to exert the tumorigenic role, IGFs derived from CAFs can confer resistance to IGF1R inhibitors as well.[155] This mechanism has been reviewed for numerous malignancies, including pancreatic and bladder cancer. [92,156]

2. Research Hypothesis and Experimental Aim

Accumulating evidence suggest that IGF1 is locally produced in several tissues, and that mesenchymal cells are a potential major source. In addition, IGF1 plays an important pro-tumorigenic role in several cancers, including bladder cancer. However, the mesenchymal-specific expression of IGF1 and its role in bladder cancer are unknown. Here, we aim to study how tissue resident mesenchymal – derived IGF1 may contribute to bladder cancer development and identify the underlying molecular pathways driving its functions. To achieve this, we will use mice with mesenchymal-specific deletion of IGF1 and an in vivo model of bladder tumorigenesis. RNA sequencing, ex vivo and in vitro experiments will be performed to delineate the molecular and cellular mechanisms that underlie the potential autocrine and paracrine functions of IGF1 in promoting bladder cancer progression.

3. Materials and Methods

3.1. Materials

3.1.1. Chemicals and Reagents

1M Tris, pH 8.0

5M NaCl

5 N HCl

0.5M EDTA, pH 8.0

10% SDS

Proteinase K (Blirt, ≥30 U/mg)

Phenol (≥99%, Fisher Scientific)

Propanol-2-ol (>99.8%, Fisher Scientific)

Absolute Ethanol (Acros Organics)

N-butyl-N-(4-hydroxybutyl) nitrosamine (BBN) (TCI Chemicals or Sigma Aldrich)

Phosphate buffered saline (Bioline)

Dulbecco's Phosphate Buffered Saline (Gibco)

Formaldehyde (PanReac AppliChem)

Hematoxylin and Eosin

OCT (VWR Chemicals)

Tri-Sodium Citrate Dihydrate (Lach:ner)

Tween 20 (Fisher Scientific)

TRITON X-100 (PanReac AppliChem)

Hydrogen Peroxide (Carlo Erba Reagents)

Albumin (Bovine Serum Albumin –BSA) Fraction V, ph 7.0 (PanReac AppliChem)

Fetal Bovine Serum (BioSera)

Penicillin, 10.000 U/mL – Streptomycin, 10.000µg/mL (Gibco)

Penicillin, 10.000 U/mL – Streptomycin, 10.000µg/mL – Antimycotic, 25µg/ml (Gibco)

Gentamycin 50ng/mL (PanReac AppliChem)

MEM Non-essential amino acids (NEAA), 100x (Gibco)

Dulbecco's Modified Eagle Medium (DMEM), 1X (Gibco)

Fibroblast Growth Supplement (Sigma Aldrich)

Recombinant mouse IGF1 protein (Abcam, ab9861)

TRItidy G (PanReac AppliChem)

Chloroform (Fisher Scientific)

oligodTs (New England Biolabs)

Moloney Murine Leukemia Virus (MMLV) Reverse Transcriptase (GeneON)

5X Reaction Buffer for MMLV (GeneON)

Taq polymerase (homemade)

dNTPs 2.5mM and 10mM (homemade)

10X Taq Buffer (homemade)

SYBR Green PCR Master Mix (Bio-rad)

Trypsin – EDTA 0.05% (1X) (Gibco)

Dimethyl sulfoxide (DMSO) (PanReac AppliChem)

Collagenase XI (Sigma Aldrich)

Dispase II (Sigma Aldrich/ROCHE)

Collagenase IV (Sigma Aldrich)

PBS with Ca^{+2}/Mg^{+2}

Acetic Acid

Crystal Violet

Methanol (Fisher Scientific)

Mounting Medium with DAPI

3.1.2. Recipes

● DMEM complete: 10% FBS, 1% NEAA, 100 U/ml penicillin, 100 µg/ml streptomycin, 1 µg/ml amphotericin B, 50 µg/mL gentamycin

● Serum Free Medium: 0.5% FBS, 1% NEAA, 100 U/ml penicillin, 100 µg/ml streptomycin, 1 µg/ml and amphotericin B

● TAIL lysis buffer: 1 M Tris, pH 8.0, 0.5 M EDTA, 5M NaCl, 10% SDS, 20 mg/mL Proteinase K

- Permeabilization Buffer: 0.2% TRITON X-100, 1X PBS
- Blocking Buffer: 1% Bovine Serum Albumin (BSA), 0,1%TRITON X, 1X PBS
- Sodium Citrate Buffer: 10mM Tri-Sodium Citrate dihydrate, 0.05% Tween 20, pH 6.0

3.1.3. Mice

Twist2-Cre mice were utilized for targeted expression of the "knocked-in" Cre recombinase in mesenchymal cells, under the control of the endogenous Twist2 promoter.[157] Twist2-Cre mice were crossed with *Igf1*$^{Lox/Lox}$ mice that bear two LoxP sequences flanking exon 4 of the *Igf1* gene.[158] (*Figure 18*) The generated Twist2cre$^{+/-}$ *Igf1*$^{Lox/Lox}$ mice (*Igf1*^{Mesko}) were used to achieve mesenchymal-specific deletion of *Igf1*. Rosa^{mTmG} reporter mice were also crossed with the above mice for cell isolation and tracing, since upon Cre induction the membrane-targeted Tomato cassette is excised, resulting in the expression of green fluorescent protein (GFP) in Cre^{+} cells (Jackson, Stock No 007676).[159] All mice were on a C57/BL6 background. All animals were maintained and bred under specific and standardized pathogen-free conditions in the "Alexander Fleming" Biomedical Sciences Research Center (BSRC) Animal Facility. Both male and female mice were included in experiments and grouped based on their sex. Co-housed littermate experimental and control mice were used in all experiments. All procedures were performed in compliance to the National Legislation and the European Legal Framework under the approval of Veterinary Service Management of the Hellenic Republic Prefecture of Attika and the guidance of the Institutional Animal Care and Use Committee of "Alexander Fleming" BSRC (License No: 49659).

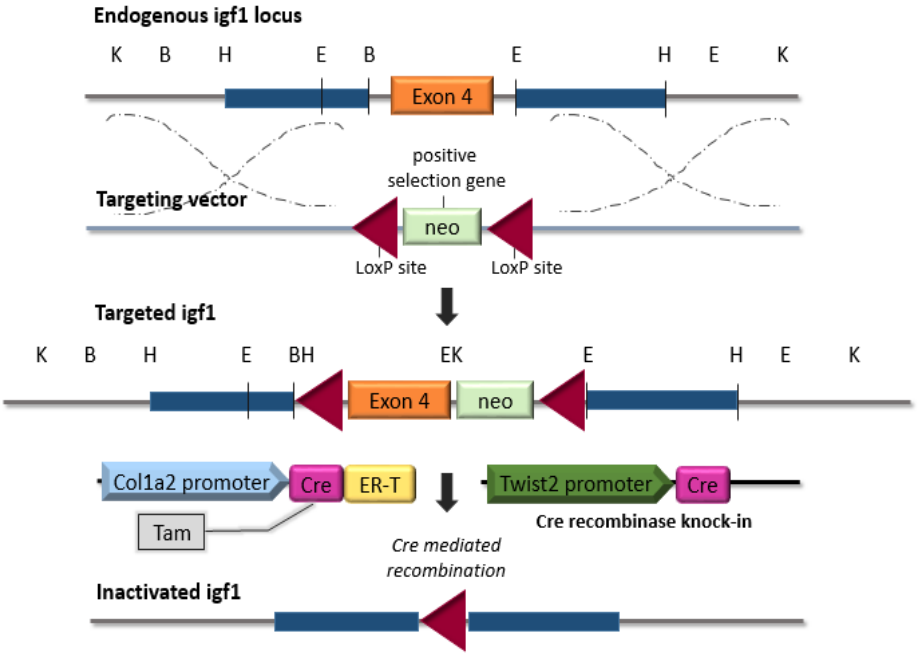

Figure 18: Illustration of mesenchymal targeted deletion of *Igf1*. Figure modified based on references 215, 216.

3.2. Methods

3.2.1. Genotyping

DNA was isolated from tail samples to verify the genotype of animals derived from crossing the Twist2-Cre strains with *Igf1*$^{Lox/Lox}$ and Rosa^{mTmG} mice. Tails were incubated in TAIL lysis Buffer (*see Recipes*) at 55^{o}C overnight. DNA was then extracted using the phenol-based method. In brief, phenol was added to the lysate in a 1:2 ratio, followed by vortex and centrifugation at 13.000rpm for 10 minutes in room temperature. The upper phase was transferred to an equal volume of isopropanol (1:1 ratio). After gentle mixing, DNA was "fished out" with a glass pipette, washed with 70% and 100% Ethanol and resuspended in 100 µl H2O. Polymerase Chain Reaction (PCR) for mouse genotyping was performed using 2 µl DNA, 2 µl Taq Buffer, 1.2 µl MgCl2 (concentration), 0,2 µl Taq polymerase and the following sets of primers (10µM each):

Table 1: PCR primer sequences for mouse genotyping.

Target	Primer	Sequence (5' → 3')
Cre	Forward	ATTACCGGTCGATGCAACGAGT
	Reverse	CAGGTATCTCTGACCAGAGTCA
mTmG	Common	CTCTGCTGCCTCCTGGCTTCT
	Wild type Reverse	CGAGGCGGATCACAAGCAATA
	Mutant Reverse	TCAATGGGCGGGGGTCGTT
Igf1	Common	CACTAAGGAGTCTGTATTTGGACC
	Mutant Forward	AAACCACACTGCTCGACATTG
	Wild type Forward	GGCAAATGGAAATCCTATGTCT

PCRs were performed on a C-1000 Touch Thermo Cycler (Bio-Rad). The cycling conditions for each PCR were:

Table 2: Genotyping PCR programs.

Igf1		**cre**		**mTmG**	
94 for 2'		94 for 4'		94 for 3'	
94 for 20''		94 for 1'		94 for 30''	

65 for 15''	*10 cycles*	57 for 1'	*5 cycles*	61 for 1'	35 cycles
68 for 10''		72 for 1'		72 for 1'	
94 for 15''	*28 cycles*	94 for 30''	*25 cycles*	72 for 5'	
60 for 15''		55 for 40''		12 for 1'	
72 for 10''		72 for 70''			
72 for 2 min		72 for 10'			
		20 for 1'			

3.2.2. Model of Muscle Invasive Bladder Cancer (MIBC)

N-butyl-N-(4-hydroxybutyl) nitrosamine (BBN) was added to the drinking water of six-week-old co-housed and littermate mice of both sexes, at a concentration of 0,05 % for 18 weeks, followed by a concentration of 0,01% for up to six additional weeks. BBN is a carcinogenic nitrosamine compound administered in vivo to model urothelial bladder cancer.[160] High grade, invasive tumors arise in the urinary bladder, resembling the histology and genetic/ alterations of human muscle invasive bladder cancer (MIBC). (*Figure 19*)

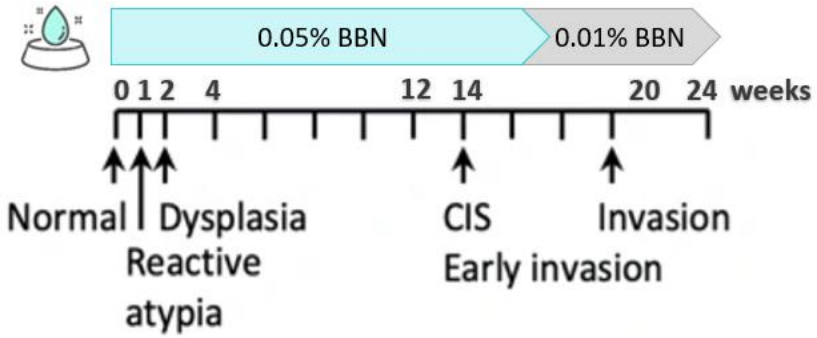

Figure 19: Timeline and stages of carcinogen-induced MIBC with the addition of differential BBN concentrations (aqua - 0.05% for 18 weeks and grey – 0.01% for up to six more weeks) in the drinking water of mice. Figure adapted based on https://translational-medicine.biomedcentral.com/articles/10.1186/s12967-019-02146-5 .

3.2.3. Ultrasound imaging

The progression of BBN-induced carcinogenesis was monitored through ultrasound imaging. This took place in the PhenoClinic of the BSRC "Alexander Fleming" Animal

House with the help of the facility's veterinarian. The equipment used was a Vevo 3100 Imaging System from FUJIFILM VisualSonics.

3.2.4. Histology

Whole urinary bladders isolated from control and knockout mice were preserved both as formalin-fixed/paraffin-embedded (FFPE) tissue blocks and as OCT-embedded frozen samples (TBS88 PARAFFIN EMBEDDING SYSTEM), according to the following procedures:

FFPE

Tissues were rinsed in 1X PBS, and fixed in 10% formalin at 4^{o}C, overnight. The following day, the tissue was washed three times in 1X PBS and treated in the Spin Tissue Processor (Leica TP1020) that enables finer sectioning of the tissue. Tissues were then coated in paraffin for long-term preservation at room temperature. Serial sections of 5 micron each were acquired with the use of a microtome (SLEE MEDICAL). Sections underwent hematoxylin and eosin (H & E) staining for histopathological evaluation. H & E stainings were observed under a Nikon E800 upright microscope.

OCT

Bladders were fixed in 4% paraformaldehyde at 4^{o}C, overnight. The next day, the organs were placed in 15% sucrose at 4^{o}C for 4 hours, followed by overnight incubation in 30% sucrose at 4^{o}C. After this fixation procedure, tissues were embedded in scaffolds filled with O.C.T. compound and snap frozen in liquid nitrogen. Samples were maintained in -80^{o}C. Tissue sectioning was performed with a Cryotome (Leica CM1950) to acquire 5-micron sections.

3.2.5. Immunohistochemistry (IHC) - Stainings

On paraffin sections

Immunostaining on paraffin sections requires wax removal (deparaffinization) and rehydration of the tissue sample. For that purpose, slides were placed in 55^{o}C for 30 minutes and immersed in xylene 3 times per 10 minutes, 100% Ethanol twice for 2 minutes, 95% Ethanol for 2 minutes, 70% Ethanol and 50% Ethanol for 1 minute each and finally in dH_2O for 1 minute. Then, slides were washed twice for 10 minutes with 1X PBS at room temperature and immersed in Sodium Citrate buffer at 60^{o}C (Microwave) for 20 minutes to achieve antigen retrieval. Afterwards, slides were rinsed with tap water and washed with 1X PBS twice for 10 minutes. Blocking of endogenous peroxidases was achieved with incubation in 0.5% Hydrogen Peroxide at room temperature for 10 minutes. After Hydrogen Peroxide was discarded, Permeabilization buffer was added for 10 minutes at room temperature. Next, blocking of non-specific staining was achieved through incubation of slides in Blocking Buffer (*see Recipes*) for 30 minutes at room temperature. Then, tissues were incubated with the primary antibodies (diluted in blocking buffer, as shown in Table 3) in humidified chambers at 4^{o}C, overnight. The following day, primary antibodies were washed away with 1X PBS and incubation with secondary antibodies (diluted in blocking buffer, as shown in "Recipes") took place at room temperature for 45

minutes, as listed in Table 3. Finally, slides were washed with 1X PBS and ddH_2O, and mounted with aqueous Mounting Medium containing DAPI for nucleus staining. Images were acquired using a Leica DM2000 Fluorescent Microscope.

On OCT sections

Once cryosections were obtained, they were left to air dry for 5 minutes at room temperature, fixed with 4% PFA for 10 minutes, and washed three times with 1X PBS for 3 minutes each. Next, sections were permeabilized by incubation in the relative buffer (*see Recipes*) for 10 minutes in room temperature, washed once with 1X PBS for 3 minutes and blocking buffer (*see Recipes*) was added for 30-40 minutes. They were subsequently incubated with the primary antibodies at 4^oC overnight, as listed in Table 3. The following day, they were washed with 1x PBS and incubated with the secondary antibodies for 45 minutes in room temperature, as shown in Table 3. Finally, they were washed with 1X PBS and dH_2O and mounted using mounting medium containing DAPI. Images were acquired using a Leica DM2000 Fluorescent Microscope.

Table 3: Antibodies used in immunohistochemistry experiments.

Primary Antibodies	**Dilutions**	**Source**	**Company**
Anti – cytokeratin5	1/1000	rabbit	Biolegend, 905501
Anti – cytokeratin8	1/300	rat	TROMA-I
Anti - IGF1R	1/1000	rabbit	Abcam, ab182408
Anti – vimentin, Alexa647	1/300	rabbit	Abcam, ab194719
APC/Cy7, Anti - CD45	1/400	rat	Biolegend, 103116
Anti - ki67	1/400	rabbit	Abcam, ab15580
FITCH – anti-actin, a – smooth muscle actin	1/400	mouse	Sigma, F3777
Alexa488, Anti - GFP	1/500	rat	Biolegend, 338007
Secondary Antibodies	**Dilutions**	**Source**	**Company**
Anti-rabbit, IgG, Alexa647	1/500	Goat	Invitrogen, A21244
Anti-mouse, IgG, Alexa488	1/500	Goat	Invitrogen, A11029
Anti-rat, IgG, Alexa568	1/500	Goat	Invitrogen, A11077

3.2.6. RNA extraction

Cultured cells

T24 human bladder cancer cells were cultured in DMEM on a 6-well plate until 60-70% confluency was reached. Then cells were serum-starved for 6h and 50ng/mL mouse recombinant IGF1 (Company) was added for 24h. Primary fibroblasts isolated from control and KO littermates were cultured in DMEM complete containing fibroblast growth supplement (FGS) on 6-well plates until the second passage. Both cell types were lysed with the addition of RLT buffer from QIAGEN RNeasy Micro Plus kit and collected using a cell scraper. RNA extraction was performed based on the manufacturer's guidelines (https://www.qiagen.com/us/products/discovery-and-translational-research/dna-rna-purification/rna-purification/total-rna/rneasy-plus-kits/).

Bladder tissue

RNA isolation from whole bladder tissues was performed using the guanidinium thiocyanate (TRIzol)-phenol-chloroform extraction method. After removal of urinary bladders, the tissues were homogenized in TRItidy G reagent that contains the guanidinium thiocyanate and phenol components. After a 5-minute incubation on ice, chloroform was added to the lysate, followed by an additional 5-minute incubation on ice. Centrifugation for 5 minutes, at 4^{o}C and 12000 rcf enabled the separation of the organic and aqueous phases with the aqueous phase retaining the extracted RNA. To precipitate the RNA, CH3COONa and 70% ice cold Ethanol were added to the upper phase in a ratio of 1:2 and 1:10 of the aqueous volume, respectively. Centrifugation for 5 minutes, at 4^{o}C and 7500 rcf enabled the precipitation of RNA. The pellet was left to air-dry and the RNA was resuspended in RNAse-free water. DNase treatment and RNA clean up procedures were performed according to the QIAGEN RNeasy Mini Plus kit guidelines (https://www.qiagen.com/us/products/discovery-and-translational-research/dna-rna-purification/rna-purification/total-rna/rneasy-plus-kits/).

3.2.7. RNA sequencing and analysis

RNA samples extracted from control untreated and BBN-treated mice were subjected to bulk 3'-mRNA sequencing. Libraries were prepared using the 3' mRNA-Seq Library Prep Kit for Ion Torrent (QuantSeq-LEXOGEN), according to the manufacturer's guidelines. The Ion PI IC200 Chef Kit (ThermoFisher) was used for template preparation on an Ion Proton Chef Instrument, and the Ion PI Sequencing 200 V3 kit and Ion Proton PI V2 Chips (ThermoFisher) were used for sequencing on an Ion Proton System, according to the manufacturer's guidelines. Sequencing and initial bioinformatic analysis was performed by the Genomic Facility of BSRC "Alexander Fleming". Downstream bioinformatic analysis was performed on lists of differentially expressed genes, using InteractiVenn for Venn diagrams (http://www.interactivenn.net/).

3.2.8. Reverse Transcription

RNA isolated from cultured cells and/or bladder tissues was subjected to reverse transcription to produce cDNA for downstream quantitative polymerase chain

reactions. 2µg RNA and 500ng/µL (80pmol/reaction) oligo-d(T)s were heated at 70 °C for 10 minutes, followed by incubation on ice for 5 minutes, addition of 5X RT Buffer, 10mM dNTPs, 200 units M-MLV (GeneOn) and RNase-free water up to 20µl and incubation at 37 °C for 1 hour and 20 minutes. cDNA samples were stored at -20 °C.

3.2.9. Quantitative / real-time polymerase chain reaction (qRT-PCR)

Gene expression in T24 human bladder cancer cell line, mouse bladder tissue, mouse bladder tumors and primary bladder fibroblasts were analyzed by qRT-PCR. *b2m* was used as house-keeping gene. cDNA (10ng/µL) was incubated with each primer set 10ng/µL (=0,2pmol/mL) and SYBR Green PCR Master Mix (Company), according to the manufacturer's instructions. Primers used for qRT-PCR, including annealing temperatures, are shown in Table 4 and Table 5 below:

Table 4: Murine qPCR primer sequences and annealing temperature.

Target	**Primer**	**Sequence (5' → 3')**	**Temperature**
Igf1	Forward	GCTGGTGGATGCTCTTCAGT	58°C
	Reverse	TCCGGAAGCAACACTCATCC	
Klk8	Forward	CCTCTTCCACCGAGTCCGA	
	Reverse	AGAAAGAATGTGAGCCTGGGG	
Krt10	Forward	GGTGACCATGCAGAACCTGA	
	Reverse	TGAGTTGCCATGCTTCTCGT	
Krt15	Forward	AGATCGGGACTACAGCCATTAC	
	Reverse	AGCCTGAAGTCGTCCGC	
S1pr1	Forward	GCCTCTCCAGCCAAGGAAAA	
	Reverse	GGAGCCTGGGGTGGTATTTC	
B2m	Forward	TTCTGGTGCTTGTCTCACTGA	
	Reverse	CAGTATGTTCGGCTTCCCATTC	

Table 5: Human qPCR primer sequences and annealing temperature.

Target	**Primer**	**Sequence (5' → 3')**	**Temperature**
KRT10	Forward	TTGAAACAATCCCTGGAAGC	
	Reverse	TATCTGGGCCTGAATCTGTG	

KRT15	Forward	CCTGAAGAAGAACCACGAAGAG	55,7°C
	Reverse	TCCATCTCCACATTGACCTG	
ADAMTS15	Forward	TCTGTCATTGAGGACGATGG	
	Reverse	ACACCTCCTCACAGACTTTCAC	
B2M	Forward	AGATGAGTATGCCTGCCGTG	
	Reverse	TCATCCAATCCAAATGCGGC	

All qRT-PCR experiments were performed in 96-well plates, on a C-1000 Touch Thermo Cycler (Bio-Rad). Data analysis was performed using the Bio-Rad CFX manager software.

3.2.10. Cell culture

T24 human bladder cancer cells (Table 6) and primary bladder fibroblasts were cultured under aseptic conditions in cell culture incubators at 37oC, and under 5% CO2 ensuring the stability of pH levels. All procedures and handling were carried out in biological safety cabinets, equipped with UV radiation lamps for sterilization. An inverted light microscope was used to observe cell morphology and growth and assess the need for passaging. Neubauer counting chambers were used to calculate cell numbers. Cell passaging was achieved with the addition of 1X Trypsin that was inactivated with the addition of DMEM complete.

Table 6: Properties of the T24 human bladder cancer cell line.

Cell line	Organism	Tissue	Morphology	Disease	Source
T24	Homo Sapiens	Bladder	Epithelial	Transitional Cell Carcinoma	Kindly provided byDr. Klinakis (BRFAA)

3.2.11. Isolation of primary bladder fibroblasts

Mice were euthanized by exposure to CO2 in combination with cervical dislocation. 2-3 urinary bladders were removed, washed in ice cold DMEM (complete) and cut longitudinally in smaller pieces. The dissected bladders were incubated at 37°C for 40 minutes in a digest buffer, containing DMEM (complete), 300 U/mL Collagenase XI and 0.1 mg/ml Dispase II. The supernatants were transferred in 10mL DMEM (complete) to dilute the enzymes and kept on ice. The remaining undigested tissue was incubated at 37°C for 20 minutes in a second digest buffer, containing DMEM (complete), 300 U/mL Collagenase XI, 0.1 mg/ml Dispase and 400 U/mL Collagenase IV. The new supernatant was pooled with the previous diluted supernatant and centrifuged at room temperature for 5 minutes in 300g. The cell pellet was resuspended in DMEM

complete containing Fibroblast Growth Supplement (FGS) and cultured in one well of a 6-well plate (passage 0). Cells were cultured until passage 2 before use.

3.2.12. Flow Cytometry

Primary mouse bladder fibroblasts were cultured as described until reaching passage 2-3. Then, cells were stained with an Alexa Fluor® 700 anti-mouse CD45 Antibody (103128, Biolegend, 1:400 dilution in FACS Buffer) for 20 minutes on ice. Stained ells were washed with FACS Buffer (1X PBS + 5% FBS) and analyzed using a BD FACS Canto II Flow Cytometer.

3.2.13. In vitro proliferation assay

T24 human epithelial bladder cancer cells were cultured in a 96-well plate at a concentration of 5 x 10^3 cells per well in DMEM complete. Once reaching 50-60% confluency, cells were cultured in serum free medium for 24 hours. Three different concentrations of mouse recombinant IGF1 (Abcam, ab9861), including 20ng/mL, 50ng/mL and 100ng/mL, was then added for 24 and 48 hours. T24 cells grown in the absence of IGF1 were used as controls. All conditions and time points were evaluated in four technical replicates. At the indicated timepoints, the supernatants were removed and cells were washed twice with 1X PBS containing Ca^{+2} and Mg^{+2}. Cells were then fixed with the addition of 100% ice cold Methanol for 10 minutes in room temperature. Methanol was discarded and cells were left to air-dry in room temperature. Crystal violet staining was added for 10 minutes, and the plate was washed under tap water and left to dry. Acetic acid 10% was added for 10 minutes to enable cell and staining resuspension. Absorbance was measured at 570nm in a Tecan Sunrise microplate reader. Analysis and graphs were produced using the GraphPad software.

3.2.14. In vitro migration assay – wound healing

T24 cells were cultured in a 48-well plate in a concentration of 0.9 x 10^5 cells per well in DMEM (Complete). Upon reaching a confluency of >90%, they were serum-starved (DMEM complete + 0.5% FBS) for 4-5 hours. The media was then discarded and a wound was created in each well with the aid of a pipette tip. Cells were washed with 1X PBS and cultured in serum free medium containing 50ng/mL mouse recombinant IGF1 for 18-24 hours. T24 cells grown in the absence of IGF1 were utilized controls. Four technical replicates were assessed for all conditions and time points. Analysis of wound healing was performed with ImageJ.

4. Results

4.1. Specificity and efficiency of *Igf1* deletion in mouse urinary bladder mesenchymal cells

The Twist2-cre and *Igf1*$^{lox/lox}$ mouse lines were utilized to achieve mesenchymal-specific deletion of *Igf1* in Twist2-expressing cells of the bladder. To define the bladder cells that express *Twist2* and *Igf1* we used publicly available RNA sequencing data.[161] We found that *Twist2* is highly expressed in all fibroblast populations and in myofibroblasts. *Igf1* is enriched in one of the fibroblast subpopulations, while it is also expressed in the other two fibroblast clusters, as well as in myofibroblasts, monocytes and neurons. Overlapping expression of *Twist2* and *Igf1* suggests that deletion is expected predominantly in bladder fibroblasts and myofibroblasts (*Figure 20*).

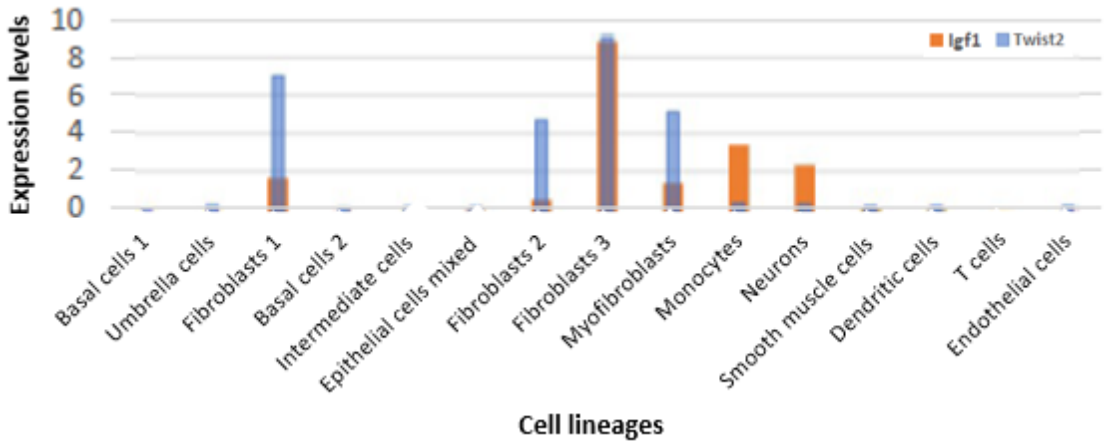

Figure 20: **Expression pattern of *Twist2* and *Igf1* in distinct bladder cell lineages.** Graphic representation of *Igf1* and *Twist2* expression levels in distinct urinary bladder cell types based on recently published data[161].

We then validated the expression pattern of *Igf1* in mouse urinary bladder cells. Urinary bladder samples were enzymatically digested and bladder epithelial (urothelial) cells and fibroblasts were isolated through FACS after staining with antibodies against Podoplanin (PDPN$^+$) for fibroblasts and epithelial cellular adhesion molecule (EpCAM$^+$) for epithelial cells. qPCR in sorted cells, as well as undigested urinary bladder, and liver as a positive control showed that *Igf1* was indeed enriched in sorted PDPN$^+$ fibroblasts, while minimally expressed in epithelial cells (*Figure 21*).

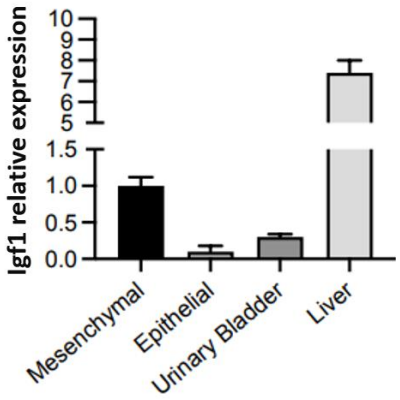

Figure 21: **Quantification of *Igf1* expression levels in the indicated cell types and tissues.** Expression in the liver is a positive control, as it is the main source of IGF1 production. The housekeeping gene *b2m* was used for normalization during data analysis.

Next, we evaluated the specificity of the Twist2-cre mouse in targeting mesenchymal cells of the urinary bladder. To this end, Twist2-cre mice were crossed with Rosa^{mTmG} reporter mice, so that cre^{+} cells express GFP and cre^{-} cells express TdTomato. We then visualized bladder tissue from Twist2^{cre}mTmG$^{Tg/Tg}$ using fluorescent microscopy, which verified that Twist2-cre expressing cells were located in the smooth muscle and subepithelial layer of the bladder. IGF1R was detected in both epithelial and mesenchymal cells (*Figure 22*).

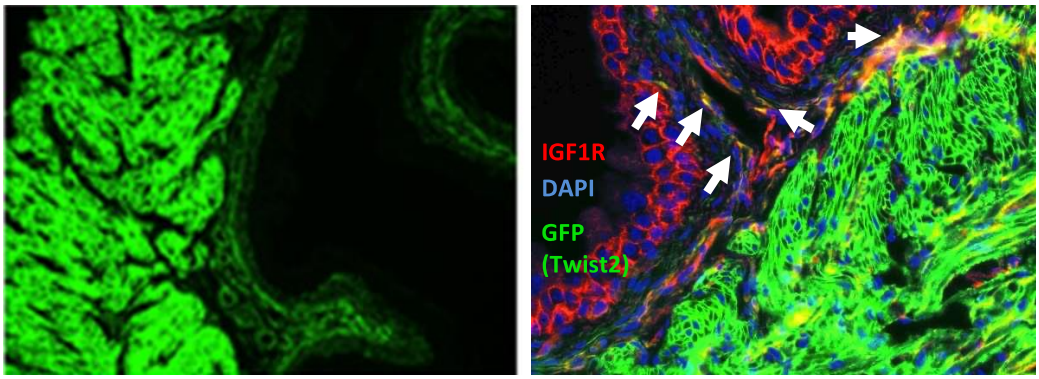

Figure 22: **Expression of GFP and IGF1R in Twist2^{cre}mTmG$^{Tg/Tg}$ mice.** Microscopy images after immunostaining with anti-GFP (green) and anti-IGF1R (red) antibody. White arrows indicate Twist2-cre+ cells that also express IGF1R.

Finally, we examined the efficiency of *Igf1* deletion in Twist2-cre cells. Twist2^{cre}*Igf1*$^{lox/lox}$ mice (hereafter *Igf1*^{Mesko}) were bred with Rosa^{mTmG} reporter mice and primary mouse urinary bladder fibroblasts were isolated and cultured. Cultured fibroblasts were stained with an antibody against CD45 and analyzed by FACS for the contamination of the culture with immune cells and the proportion of Twist2^{+} fibroblasts (*Figure 23*). After validating the purity (8.1% CD45^{+} cells) and adequate presence of Twist2^{+} cells (79.8% of CD45^{-} cells) in our cultures, we performed qPCR to analyze the expression of *Igf1* in isolated fibroblasts from control and *Igf1*^{Mesko} mice.

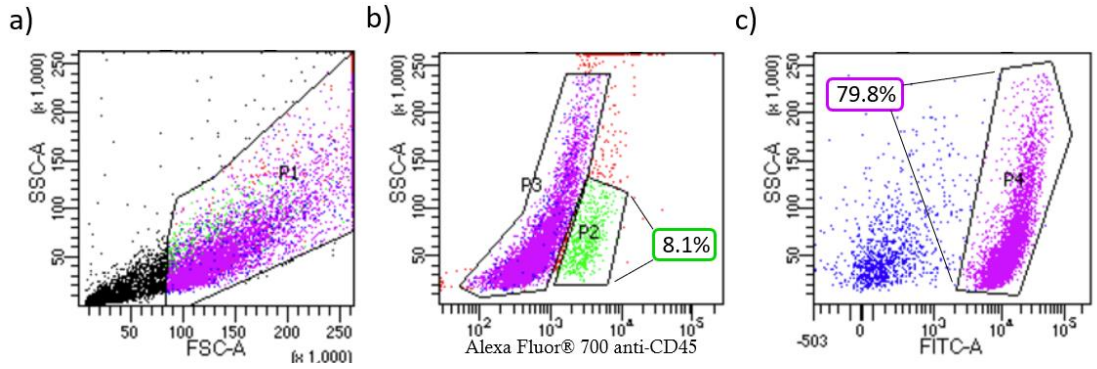

Figure 23: Flow cytometry analysis of cultured bladder fibroblasts from *Igf1*^{Mesko}-mTmG mice. a) FACS plot of side-scatter (SSC-A) and forward-scatter (FSC-A) detection. Cells depicted as black dots represent dead cells and debris excluded from the analysis. **b)** FACS plot depicting cells stained with Alexa-Fluorophore 700 anti-CD45 antibody. CD45$^+$ cells correspond to 8.1% of cultured cells (P2). **c)** FACS plot depicting GFP$^+$ mesenchymal cells. GFP$^+$ cells (P4) correspond to 79.8% of CD45$^-$ cells (P3).

We found that *Igf1* was reduced by 50% in cultures from conditional knockout mice, which accounts for approximately 70% deletion in Twist2$^+$ cells (*Figure 24*). In sum, we verified the specificity of the Twist2-cre mouse for bladder mesenchymal cells and the efficient deletion of *Igf1* in these cells.

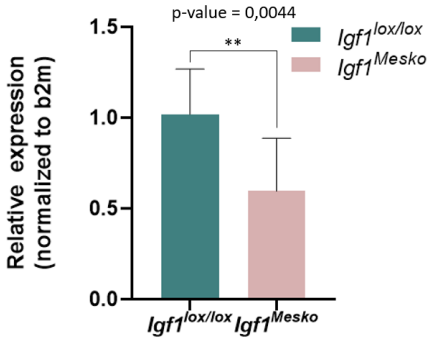

Figure 24: *Igf1* deletion in bladder mesenchymal cells. *Igf1* expression levels normalized based on the expression of the b2m gene in cultured fibroblasts isolated from *Igf1*$^{lox/lox}$ and *Igf1*^{Mesko} mice (n=3 per genotype). Statistical significance was calculated with the Wilcoxon's paired t-test.

4.2. Deletion of *Igf1* in mesenchymal cells exacerbates mouse bladder tumorigenesis

To examine the effect of mesenchymal-specific *Igf1* deletion in bladder carcinogenesis, we utilized the BBN mouse model of carcinogen-induced bladder cancer that mimics human muscle invasive urothelial cancer.[220] 6-week old *Igf1*^{Mesko} mice and littermate *Igf1*$^{lox/lox}$ controls were treated with 0.05% BBN for 18 weeks to reach the stage of *carcinoma in situ* and early invasion, as shown in *Figure 25*. Reduced

concentration of 0.01% BBN was administered in the drinking water for up to six additional weeks until muscle invasion was present.

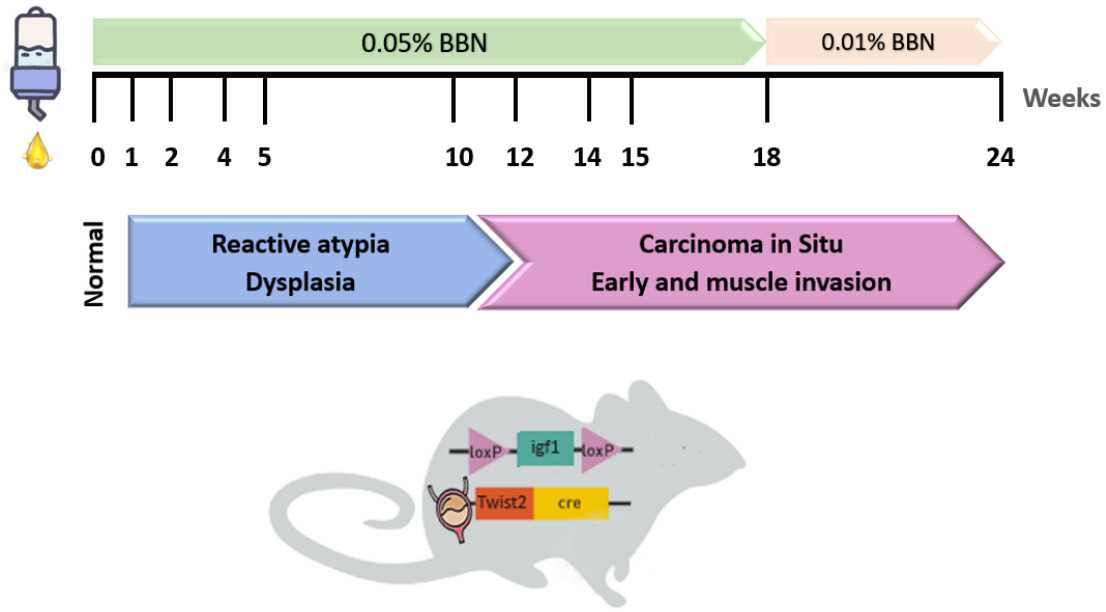

Figure 25: **Schematic representation of the BBN-induced muscle invasive urinary bladder mouse model.** *Igf1*^{Mesko}mice and *Igf1*$^{lox/lox}$ littermate control animals were administered BBN in the drinking water for a period of 25 weeks. For the first 18 weeks mice received 0.05% BBN, followed by reduced 0.01% BBN concentration for up to 6 weeks.

Bladder tumor progression was monitored through ultrasound imaging at the 19th and 21st week of the protocol (*Figure 26*a). The size of both bladders and tumors were measured and *Igf1*^{Mesko} mice showed lower tumor to bladder ratio in comparison to control mice, although it did not reach statistical significance, possibly due to high variability between mice (*Figure 26b*). However, macroscopic and histopathological evaluation of urinary bladders at 21-24 weeks revealed a significant decrease in tumor volume in *Igf1*^{Mesko} (*Figure 27a*, c). In addition, histopathological evaluation of urinary bladders showed significantly reduced histological score and invasion incidence in *Igf1*^{Mesko} mice, where the tumors were restricted behind the muscle layer of the detrusor (*Figure 27b, d, e*). Overall, our results suggest that mesenchymal-specific IGF1 have a tumor-promoting role in bladder cancer, and especially in cancer invasiveness.

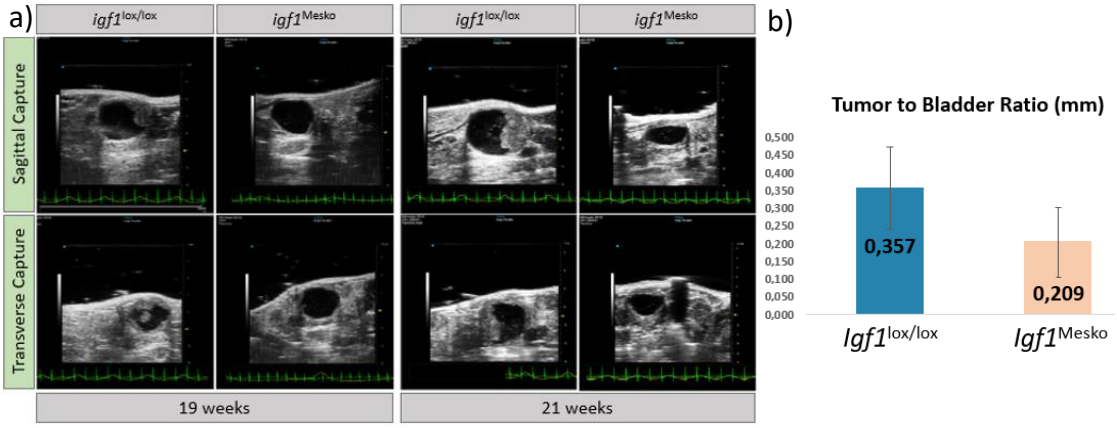

Figure 26: Ultrasound imaging and tumor measurements in BBN-treated control and Igf1^{Mesko} mice. **a)** Ultrasound imaging of the BBN-treated *Igf1*$^{lox/lox}$ and *Igf1*^{Mesko} mice. Images were acquired as sagittal and transverse captures at 19- and 21-weeks post initiation of BBN administration. **b)** Mean tumor/bladder ratio measured during ultrasound imaging at 21 weeks (n=7 mice per genotype).

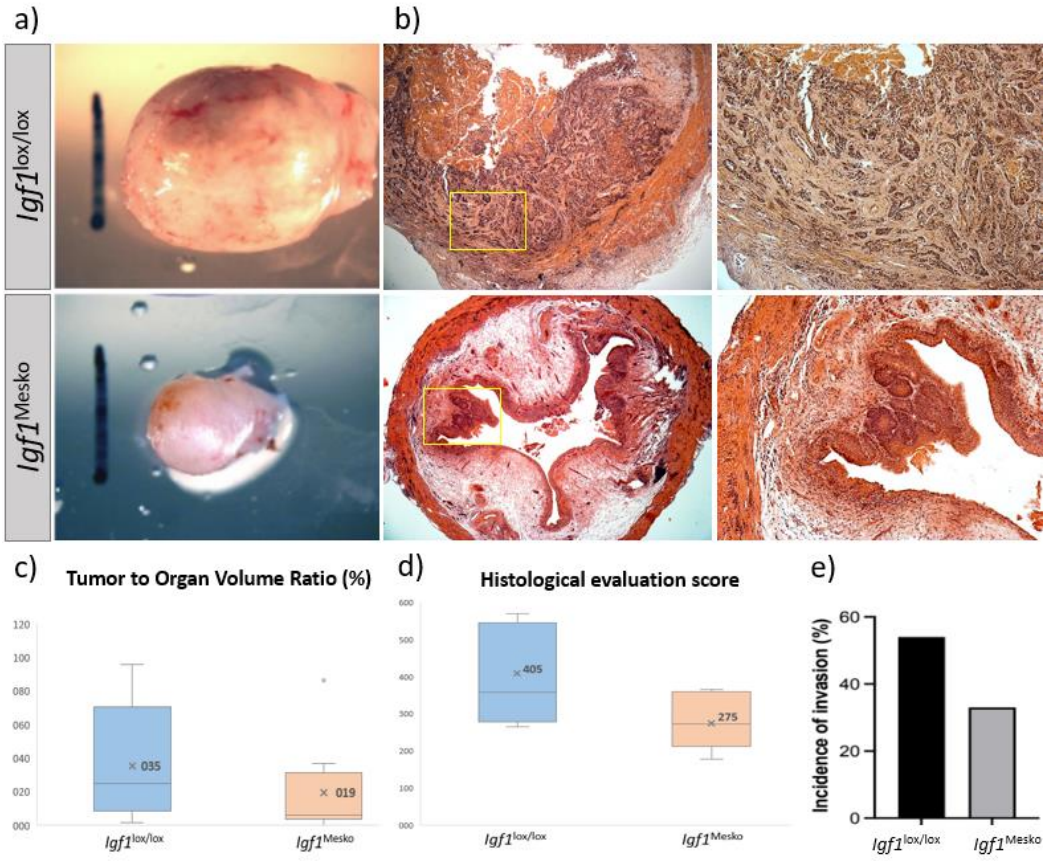

Figure 27: **Macroscopic and histopathological evaluation of BBN-treated control and *Igf1*^{Mesko} bladders. a)** Macroscopic evaluation of urinary bladders and **b)** hematoxylin and eosin (H&E) staining of tissue sections from BBN-treated *Igf1*$^{lox/lox}$ and *Igf1*^{Mesko} mice**. c)** Tumor to organ volume ratio, **d)** histological score and **e)** invasion incidence calculated in H&E stained tissue sections from *Igf1*$^{lox/lox}$ and *Igf1*^{Mesko} (n= 13-17 mice per genotype).

4.3. Immunohistochemical characterization of cancer-related properties in *Igf1*^{Mesko} mice

To further characterize the properties of tumors with mesenchymal-specific deletion of *Igf1*, we performed immunohistochemical staining on bladder tissue sections with specific cellular markers. Cytokeratin 5 (CK5) and Cytokeratin 8 (CK8) were assessed to define the basal/stem and luminal bladder epithelial cells, respectively. A-SMA and Vimentin were evaluated as markers of cells with mesenchymal origin, including activated fibroblast populations and smooth muscle cells.

CK5$^+$ stem cells were localized in the basal layer, while CK8$^+$ luminal cells in the apical surface of the urothelium both in *Igf1*$^{lox/lox}$ control and *Igf1*^{Mesko} mice. However, CK5$^+$ migrating cells were only found intermingled within the muscularis layer in *Igf1*$^{lox/lox}$ tumorous bladders, while invasion in the muscular layer was absent in *Igf1*^{Mesko} mice. This indicates that mesenchymal-specific abrogation of *Igf1* expression is responsible for reduced tumor cell migration in the muscle layer and thus less aggressive tumor development and is in agreement with the histopathological analysis. (*Figure 28a*)

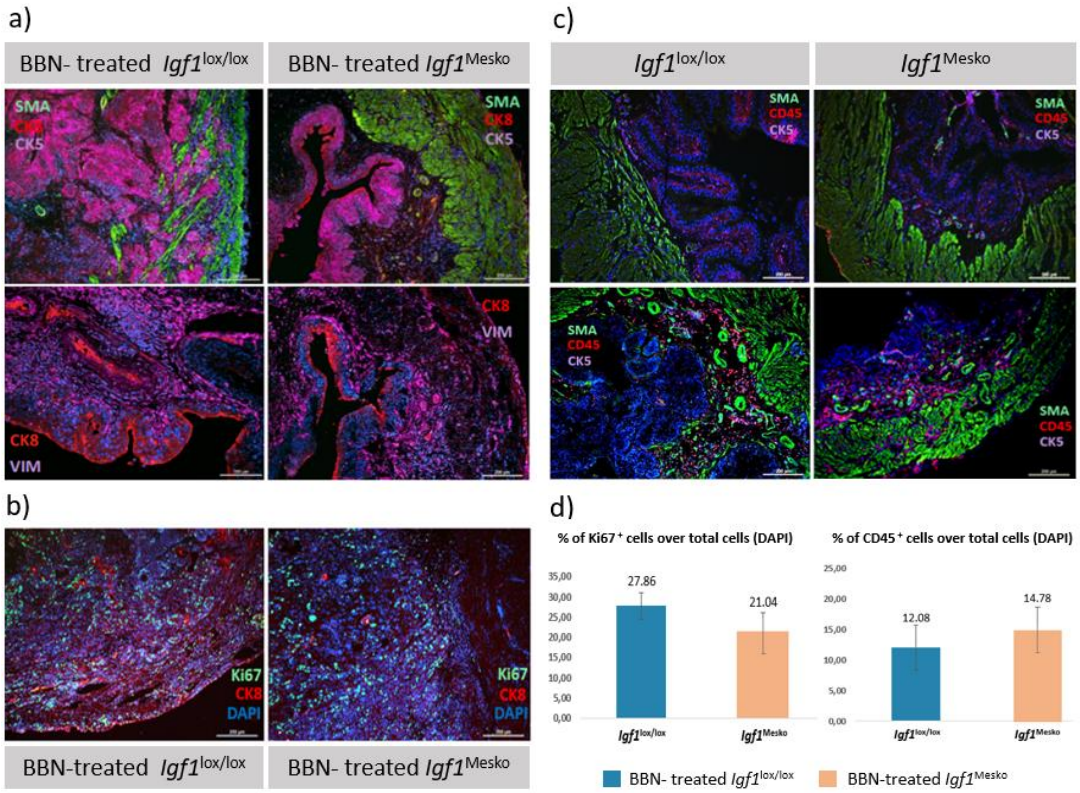

Figure 28: **Immunostaining of normal and tumor-bearing urinary bladders from *Igf1*$^{lox/lox}$ and *Igf1*^{Mesko} mice. a)** Antibodies against a-smooth muscle actin (a-SMA) and Vimentin were utilized to visualize mesenchymal cells, cytokeratin8 (CK8) for epithelial luminal cells and cytokeratin5 (CK5) for epithelial basal/stem cells in urinary bladder tumors. **b)** Immunohistochemical staining of the Ki67 proliferation marker in bladder tumor sections from *Igf1l*$^{lox/lox}$ and *Igf1*^{Mesko}mice. **c)** Immunostaining of CD45$^+$ immune cells in untreated healthy bladders and BBN-treated cancerous bladders from control *Igf1*$^{lox/lox}$ and *Igf1*^{Mesko}

mice. **d)** Quantification of Ki67 positive proliferating cells (n=6 mice per group) and $CD45^+$ immune cells (n=3 mice per group) in sections from *Igf1l*$^{lox/lox}$ and *Igf1*^{Mesko} mice.

Staining against Ki67 was performed to characterize the proliferative capacity of bladder cell populations in homeostasis and cancer. Quantification of Ki67+ cells did not show significant differences in cell proliferation between the two genotypes (*Figure 28b, d*). To characterize immune cell infiltration, we also performed immunostaining for $CD45^+$ immune cells, which also did not reveal significant differences in the numbers of recruited immune cells (*Figure 28c, d*). In sum, immunohistochemical analysis of bladder tumors from *Igf1*^{Mesko} mice showed a significant reduction in the invasion of CK5+ basal/stem cells in the muscularis layer, while there was no significant difference in immune cell infiltration and proliferation.

4.4. Expression profile of tumors with mesenchymal-specific *Igf1* deletion

To identify the molecular mechanisms underlying the reduced tumorigenesis of *Igf1*^{Mesko} mice, we performed high-throughput bulk RNA sequencing. Healthy bladders from untreated control (*Igf1*$^{lox/lox}$/*Igf1*^{Mesko}) and cancerous bladders from the BBN-treated control and *Igf1*^{Mesko} mice were processed for RNA isolation and subsequent 3' mRNA sequencing analysis.

Pairwise sample correlation was estimated based on the read counts acquired by RNA sequencing through the metaseqR2 pipeline.[162] The correlation plot revealed two distinct grouped clusters. All BBN-treated samples were clustered together, while all untreated samples were grouped separately. Each cluster revealed a high within group correlation index. The outcome is expected when comparing healthy normal bladders with BBN-treated samples (*Figure 29a*). Similar results were also obtained by performing multidimensional scaling (MDS). In the MDS plots, untreated control samples (green squares) cluster together and are similar. Accordingly, BBN-treated samples also cluster together. However, samples from *Igf1*^{Mesko} mice (red squares) are closely correlated, while BBN-treated control (*Igf1*$^{lox/lox}$) samples appear to have high variability (*Figure 29b*).

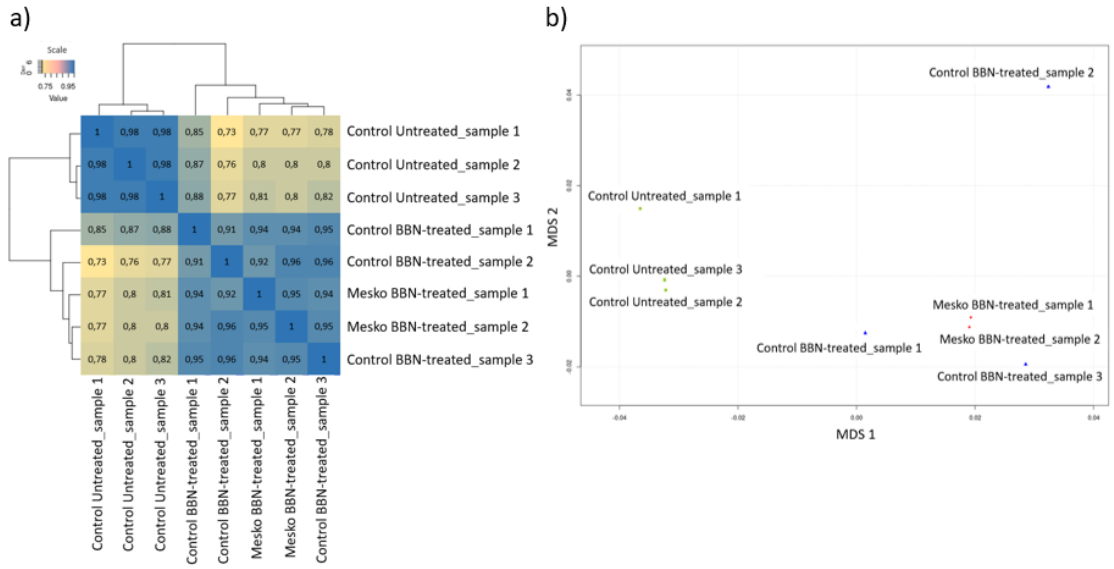

Figure 29: **Correlation and variability assessment in bulk RNA sequencing. a)** Pairwise sample correlation matrix of RNA-seq samples based on read counts. Blue color corresponds to higher correlation (max value=1) and yellow color to lower correlation (min value=0,73). **b)** Multidimensional scaling (MDS) plot revealing the correlation and reproducibility between samples in RNA sequencing analysis.

After analysis of the statistically significant deregulated genes, we found 98 genes downregulated and 121 genes upregulated in *Igf1*^{Mesko} versus control tumors (*Figure 30a*). To further narrow down the list of deregulated genes we also compared genes downregulated in *Igf1*^{Mesko} tumors versus genes overexpressed in control tumors in comparison to normal samples (*Figure 30b*). Common genes (*Figure 30b*) have significantly elevated expression in bladder cancer and are downregulated in the absence of *Igf1*. Genes of interest are shown in *Figure 30c*.

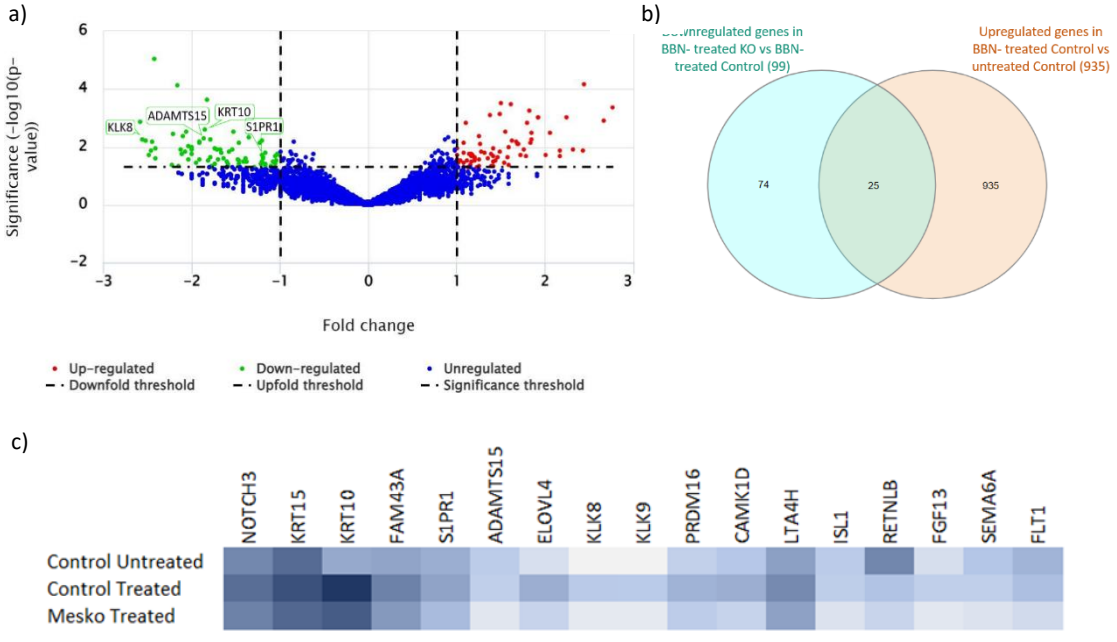

Figure 30: Characterization of genes significantly downregulated in *Igf1*^{Mesko} mice. a) Volcano plot depicting genes with significantly altered expression in tumors of BBN-treated *Igf1*^{Mesko} mice in comparison to tumors from BBN-treated *Igf1*$^{lox/lox}$ control mice. Red dots correspond to genes with significantly elevated expression, while green dots represent genes with significantly decreased expression. Blue dots depict genes with unaltered or not-significantly altered expression. **b)** Venn Diagram depicting the number of downregulated genes in BBN-treated *Igf1*^{Mesko} mice versus BBN-treated control *Igf1*$^{lox/lox}$ (blue) in comparison with genes upregulated in control tumors (BBN-treated *Igf1*$^{lox/lox}$) versus healthy normal controls (orange). **c)** Heatmap depicting expression levels of selected significantly downregulated genes in BBN-treated *Igf1*^{Mesko}. Differential gene expression is visualized as color gradient among all murine sample types used in RNA sequencing. Dark blue corresponds to higher expression and light blue to lower expression levels.

We focused on these genes, since they correspond to genes upregulated in invasive urinary bladder cancer and could be involved in the ameliorated cancer phenotype of *Igf1*^{Mesko} mice. We then used database search and literature mining to select potentially important genes for downstream validating qPCRs and functional analysis. The Human Protein Atlas (HPA) and cbioportal (https://www.proteinatlas.org/ , https://www.cbioportal.org/) were used to identify genes annotated as prognostic markers in bladder urothelial carcinoma. S1PR1, KLK8, ADAMTS15 were identified as unfavorable prognostic markers with higher expression indicating poorest survival rates (*Figure 31*). KRT10 and KRT15 are markers of cellular migration and invasion of urothelial cells. As such, the expression of these genes in 3 different *Igf1*^{Mesko} and *Igf1*$^{lox/lox}$ tumors was further evaluated with qPCR, which showed a decrease only in *Krt10*, *Krt15* and *Klk8* expression levels, although it did not reach statistical significance. This could be due to the small number of samples and increased variability especially in the control tumors. (*Figure 32*). *S1pr1*, as well as *Igf1* levels were not altered. For *Igf1*, this suggests that other sources could compensate for the mesenchymal-specific deletion and that the phenotypic differences that we observe could be due to location-specific cell interactions.

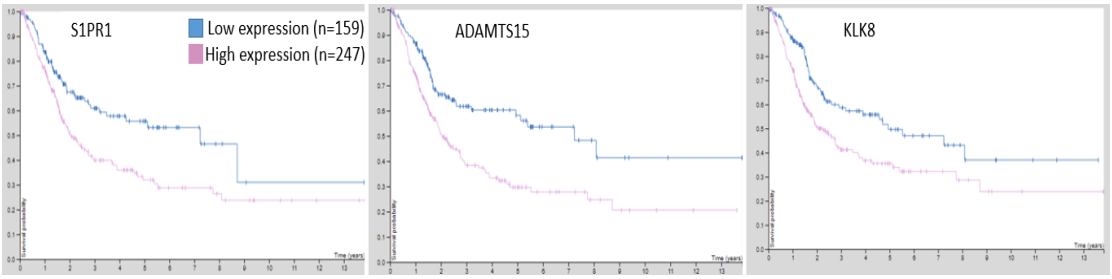

***Figure 31**:* **Prognostic markers in bladder urothelial carcinoma.** Kaplan Maier survival plots derived from Human Protein Atlas (HPA) consortium. Survival probability plots of urothelial bladder cancer patients depict *KLK8*, *S1PR1* and *ADAMTS15* as unfavorable prognostic markers in urothelial carcinoma. High expression (pink) of these genes has significant (p-values<0.001) association with urinary bladder cancer patient survival.

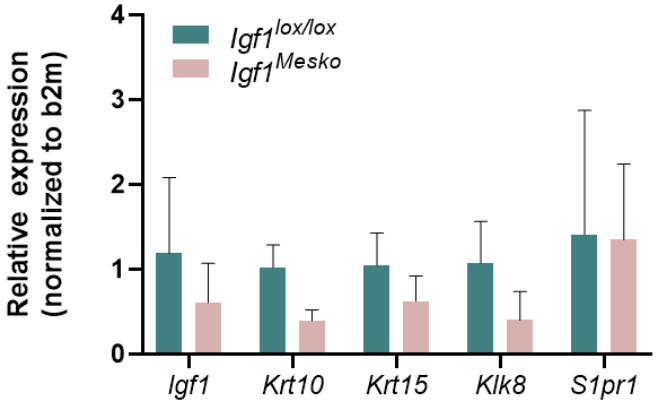

Figure 32: **qPCR validation of selected gene expression levels in *Igf1*^{Mesko} mice.** qPCR analysis of the expression levels of *Igf1*, *Krt10*, *Krt15*, *Klk8*, *S1pr1* in bladders from BBN-treated control *Igf1*$^{lox/lox}$ and *Igf1*^{Mesko} mice (n=3 mice per genotype).

4.5. In vitro effect of *Igf1* on bladder cancer epithelial cells

In vitro functional experiments were performed with T24 human bladder cancer cell line to identify stromal-epithelial cancer cell interactions. First, the proliferative capacity of T24 was assessed in control untreated conditions and following exogenous treatment with different concentrations of mouse recombinant IGF1. The analysis indicated the expected increase in proliferation of both control and IGF1-induced cells 24 and 48 hours after initiation. However, there was no significant alteration in T24 cellular proliferation under exogenous IGF1 induction, in comparison to normal untreated cells. (*Figure 33*)

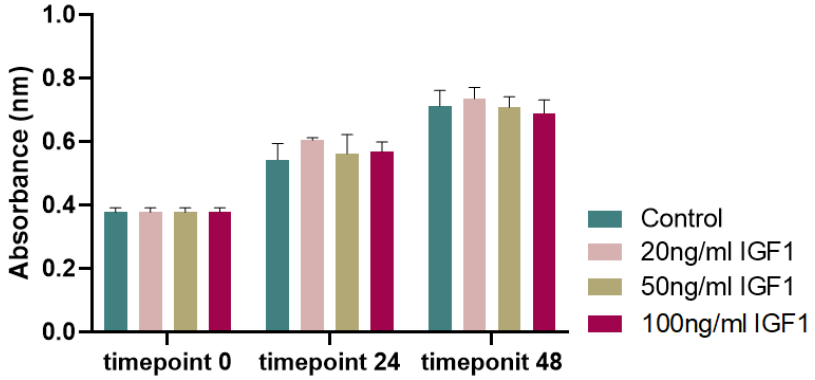

Figure 33: **In vitro assessment of proliferation in T24 human bladder cancer cells.** Graph showing T24 bladder cancer cell proliferation under control untreated conditions and exogenous IGF1 induction. Cells were treated with 20ng/ml, 50ng/ml and 100ng/ml mouse recombinant IGF1 in quadruplicates (representative of 3 experiments).

Next, we evaluated the effect of exogenous IGF1 upon migration of T24 cells. In vitro wound healing was assessed 24 hours after incubation with 20ng/ml and 50ng/ml mouse recombinant IGF1 and the wound area was measured at both timepoints (initiation-0h and 24h). Microscopy images and quantifications did not show significant differences in the migratory capacity of untreated and IGF1-treated T24 cells (*Figure 34*).

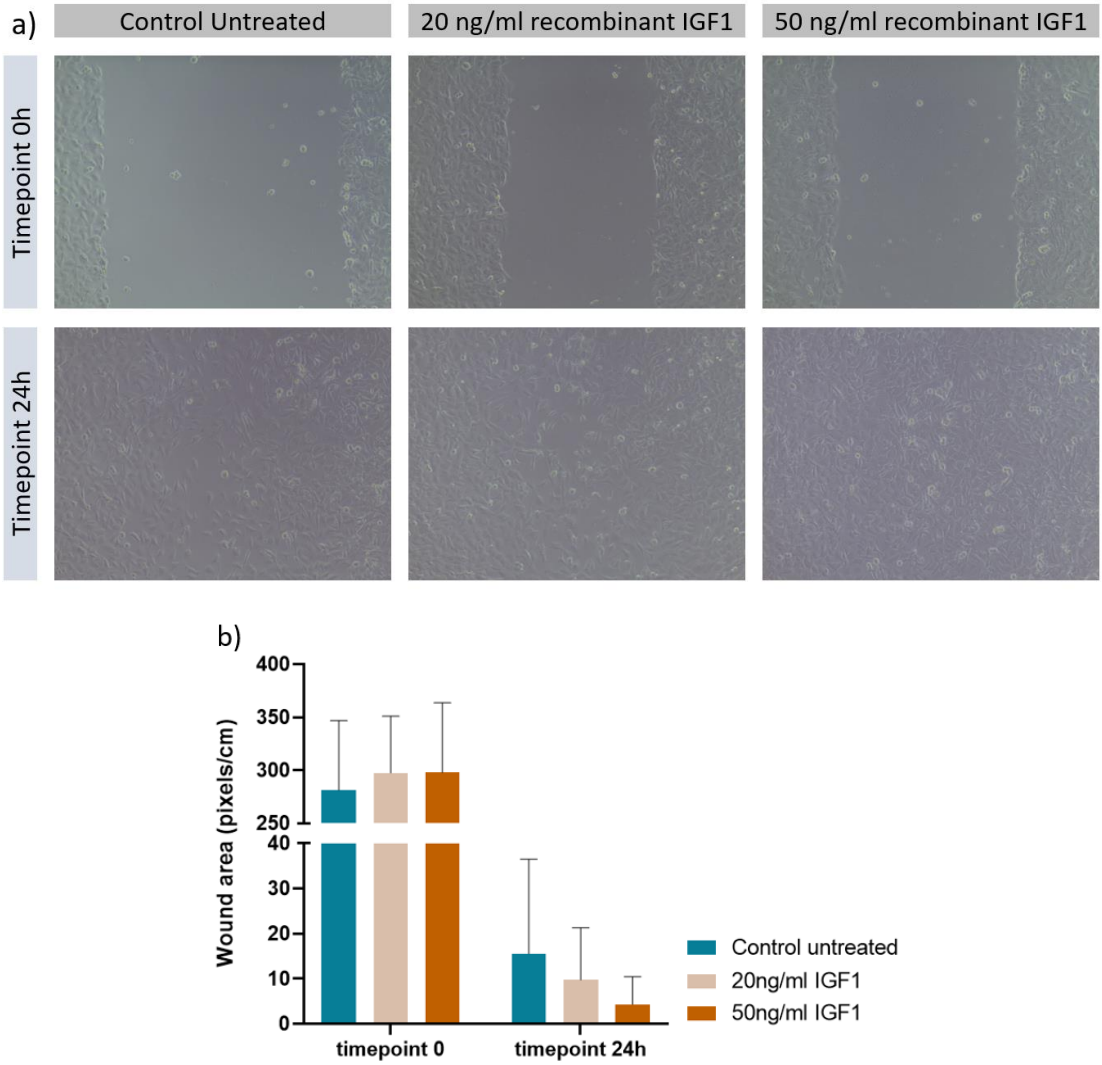

Figure 34: **In vitro wound healing assessment in T24 human bladder cancer cells. a)** Light-microscope images of T24 control untreated cells and T24 cells treated with 20ng/ml and 50ng/ml mouse recombinant IGF1 at 0 and 24h. **b)** Graph depicting quantification of the wound area at the initiation of the experiment (timepoint 0) and 24h following wound creation (representative of 5 experiments).

We also measured the expression levels of previously identified genes of interest, including *KRT10, KRT15* and *ADAMTS15* following exogenous IGF1 induction of T24 cells and found no significant difference (*Figure 35*). Overall, our in vitro results did not reveal a direct effect on IGF1 on epithelial cell proliferation, migration and cancer-related gene expression.

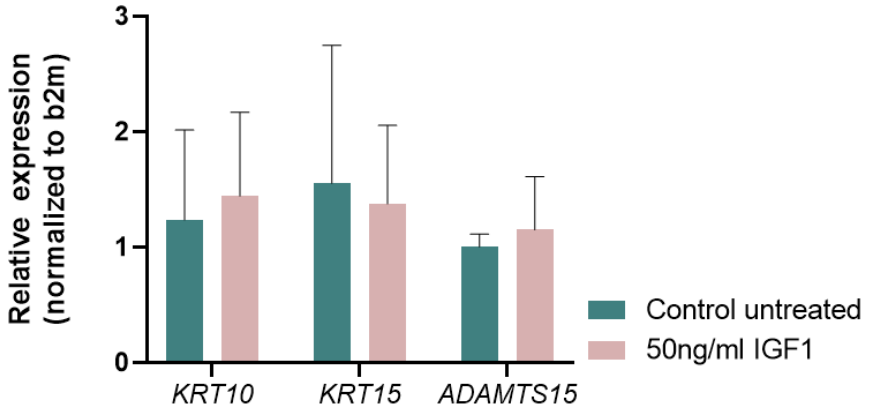

Figure 35: Expression levels of selected genes in T24 human bladder cancer cells. qPCR analysis of the expression levels of *KRT10*, *KRT15*, *ADAMTS15* in T24 human bladder cancer cells in control untreated conditions and following induction with 50 ng/ml mouse recombinant IGF1 (n=3 biological replicates per condition).

Discussion

Given the pro-proliferative and tumor-promoting role of the IGF1/IGF1R axis in cancer, better understanding of the cellular sources and molecular mechanisms underlying the functions of IGF1 in particular cancer types could enable more effective and targeted therapeutic approaches. [163]In this study, we showed that IGF1 can also be expressed by mesenchymal cells in the urinary bladder and bladder tumors, apart from its predominant synthesis in the liver. Therefore, its potential localized function in the crosstalk between mesenchymal stromal cells and cancer cells could be crucial for the establishment and progression of malignant transformation. To address this hypothesis, we utilized the BBN-induced bladder cancer mouse model to examine the role of locally produced IGF1 in muscle-invasive bladder cancer pathology. Mesenchymal specific deletion of Igf1 resulted in a decrease of tumor volume and significant reduction of cytokeratin 5^+ cancer cell migration and invasion in the muscle layer, while cell proliferation and immune cell infiltration were not affected. This comes in agreement with recent findings on stromal-derived IGF1 being implicated in the promotion of metastatic mechanisms in other types of cancer, especially in pancreatic ductal adenocarcinoma (PDAC). [156]

Analysis of the gene expression profile of bladder tumors lacking mesenchymal-specific IGF1 revealed reduced expression of genes upregulated in bladder tumor samples versus normal bladder tissue. These included genes with annotated prognostic value in bladder cancer and markers of cell migration, such as Krt10, Krt15, S1pr1, Adamts15 and Klk8. However, Igf1 total levels were not altered in Igf1Mesko, suggesting that there are additional cellular sources for IGF1, which could compensate for the mesenchymal-specific deletion and could thus mask an ever more pronounced

amelioration. This result also indicated that the phenotypic difference that we show is most possibly due to location-specific cell interactions driving cell migration.

To examine whether IGF1 can directly induce such effects on cancer cells, we performed in vitro experiments using the T24 bladder cancer cell line. However, we did not find any difference in cancer cell proliferation and migration, or the expression of previously selected genes in response to IGF1 stimulation. This might be to the potential unsuitability of the cell line, and further repetition of these experiments in other bladder cancer cell lines or primary mouse bladder cell cultures should be performed to verify the lack of an effect. If true, these results could suggest that either IGF1 has other unidentified effects on cancer cells or that its role on cancer progression is indirect through its functions in other cell types. To address this, it would be interesting in the future to examine the cell-specific role of its receptor (IGF1R) in bladder tumorigenesis and identify the downstream molecular mechanisms that regulate cancer cell functions in this setting.

References

1 Abraham, S. N. & Miao, Y. The nature of immune responses to urinary tract infections. *Nat Rev Immunol* **15**, 655-663 (2015). https://doi.org:10.1038/nri3887

2 Ajalloueian, F., Lemon, G., Hilborn, J., Chronakis, I. S. & Fossum, M. Bladder biomechanics and the use of scaffolds for regenerative medicine in the urinary bladder. *Nat Rev Urol* **15**, 155-174 (2018). https://doi.org:10.1038/nrurol.2018.5

3 Andersson, K. E. & McCloskey, K. D. Lamina propria: the functional center of the bladder? *Neurourol Urodyn* **33**, 9-16 (2014). https://doi.org:10.1002/nau.22465

4 Borsdorf, M. *et al.* Locational and Directional Dependencies of Smooth Muscle Properties in Pig Urinary Bladder. *Front Physiol* **10**, 63 (2019). https://doi.org:10.3389/fphys.2019.00063

5 Ferlay, J. *et al.* Cancer statistics for the year 2020: An overview. *Int J Cancer* (2021). https://doi.org:10.1002/ijc.33588

6 Bray, F. *et al.* Global cancer statistics 2018: GLOBOCAN estimates of incidence and mortality worldwide for 36 cancers in 185 countries. *CA Cancer J Clin* **68**, 394-424 (2018). https://doi.org:10.3322/caac.21492

7 Gu, J. & Wu, X. Genetic susceptibility to bladder cancer risk and outcome. *Per Med* **8**, 365-374 (2011). https://doi.org:10.2217/pme.11.15

8 Wong, M. C. S. *et al.* The global epidemiology of bladder cancer: a joinpoint regression analysis of its incidence and mortality trends and projection. *Sci Rep* **8**, 1129 (2018). https://doi.org:10.1038/s41598-018-19199-z

9 Teoh, J. Y. *et al.* Global Trends of Bladder Cancer Incidence and Mortality, and Their Associations with Tobacco Use and Gross Domestic Product Per Capita. *Eur Urol* **78**, 893-906 (2020). https://doi.org:10.1016/j.eururo.2020.09.006

10 Cacciamani, G. E. *et al.* Association between Smoking Exposure, Neoadjuvant Chemotherapy Response and Survival Outcomes following Radical Cystectomy:

Systematic Review and Meta-Analysis. *J Urol* **204**, 649-660 (2020). https://doi.org:10.1097/JU.0000000000000813
11 Burger, M. *et al.* Epidemiology and risk factors of urothelial bladder cancer. *Eur Urol* **63**, 234-241 (2013). https://doi.org:10.1016/j.eururo.2012.07.033
12 Berdik, C. Unlocking bladder cancer. *Nature* **551**, S34-S35 (2017). https://doi.org:10.1038/551S34a
13 Chalasani, V., Chin, J. L. & Izawa, J. I. Histologic variants of urothelial bladder cancer and nonurothelial histology in bladder cancer. *Can Urol Assoc J* **3**, S193-198 (2009). https://doi.org:10.5489/cuaj.1195
14 Tavora, F. & Epstein, J. I. Bladder cancer, pathological classification and staging. *BJU Int* **102**, 1216-1220 (2008). https://doi.org:10.1111/j.1464-410X.2008.07962.x
15 Gaisa, N. T. *et al.* Different immunohistochemical and ultrastructural phenotypes of squamous differentiation in bladder cancer. *Virchows Arch* **458**, 301-312 (2011). https://doi.org:10.1007/s00428-010-1017-2
16 Holmäng, S. & Johansson, S. L. The nested variant of transitional cell carcinoma--a rare neoplasm with poor prognosis. *Scand J Urol Nephrol* **35**, 102-105 (2001). https://doi.org:10.1080/003655901750170425
17 Trabelsi, A. *et al.* Micropapillary carcinoma of the urinary bladder: a case report and review of the literature. *Can Urol Assoc J* **2**, 540-542 (2008). https://doi.org:10.5489/cuaj.925
18 Knowles, M. A. & Hurst, C. D. Molecular biology of bladder cancer: new insights into pathogenesis and clinical diversity. *Nat Rev Cancer* **15**, 25-41 (2015). https://doi.org:10.1038/nrc3817
19 Tran, L., Xiao, J. F., Agarwal, N., Duex, J. E. & Theodorescu, D. Advances in bladder cancer biology and therapy. *Nat Rev Cancer* **21**, 104-121 (2021). https://doi.org:10.1038/s41568-020-00313-1
20 Teoh, J. Y. *et al.* Recurrence mechanisms of non-muscle-invasive bladder cancer - a clinical perspective. *Nat Rev Urol* (2022). https://doi.org:10.1038/s41585-022-00578-1
21 Park, J. C., Citrin, D. E., Agarwal, P. K. & Apolo, A. B. Multimodal management of muscle-invasive bladder cancer. *Curr Probl Cancer* **38**, 80-108 (2014). https://doi.org:10.1016/j.currproblcancer.2014.06.001
22 Lopez-Beltran, A. *et al.* Immune Checkpoint Inhibitors for the Treatment of Bladder Cancer. *Cancers (Basel)* **13** (2021). https://doi.org:10.3390/cancers13010131
23 Baghban, R. *et al.* Tumor microenvironment complexity and therapeutic implications at a glance. *Cell Commun Signal* **18**, 59 (2020). https://doi.org:10.1186/s12964-020-0530-4
24 Junttila, M. R. & de Sauvage, F. J. Influence of tumour micro-environment heterogeneity on therapeutic response. *Nature* **501**, 346-354 (2013). https://doi.org:10.1038/nature12626
25 Denton, A. E., Roberts, E. W. & Fearon, D. T. Stromal Cells in the Tumor Microenvironment. *Adv Exp Med Biol* **1060**, 99-114 (2018). https://doi.org:10.1007/978-3-319-78127-3_6
26 Koliaraki, V., Prados, A., Armaka, M. & Kollias, G. The mesenchymal context in inflammation, immunity and cancer. *Nat Immunol* **21**, 974-982 (2020). https://doi.org:10.1038/s41590-020-0741-2
27 Plikus, M. V. *et al.* Fibroblasts: Origins, definitions, and functions in health and disease. *Cell* **184**, 3852-3872 (2021). https://doi.org:10.1016/j.cell.2021.06.024
28 D'Arcangelo, E., Wu, N. C., Cadavid, J. L. & McGuigan, A. P. The life cycle of cancer-associated fibroblasts within the tumour stroma and its importance in disease

outcome. *Br J Cancer* **122**, 931-942 (2020). https://doi.org:10.1038/s41416-019-0705-1
29 Kalluri, R. The biology and function of fibroblasts in cancer. *Nat Rev Cancer* **16**, 582-598 (2016). https://doi.org:10.1038/nrc.2016.73
30 Gomes, R. N., Manuel, F. & Nascimento, D. S. The bright side of fibroblasts: molecular signature and regenerative cues in major organs. *NPJ Regen Med* **6**, 43 (2021). https://doi.org:10.1038/s41536-021-00153-z
31 Sahai, E. *et al.* A framework for advancing our understanding of cancer-associated fibroblasts. *Nat Rev Cancer* **20**, 174-186 (2020). https://doi.org:10.1038/s41568-019-0238-1
32 Ping, Q. *et al.* Cancer-associated fibroblasts: overview, progress, challenges, and directions. *Cancer Gene Ther* **28**, 984-999 (2021). https://doi.org:10.1038/s41417-021-00318-4
33 LeBleu, V. S. & Kalluri, R. A peek into cancer-associated fibroblasts: origins, functions and translational impact. *Dis Model Mech* **11** (2018). https://doi.org:10.1242/dmm.029447
34 Bu, L. *et al.* Biological heterogeneity and versatility of cancer-associated fibroblasts in the tumor microenvironment. *Oncogene* **38**, 4887-4901 (2019). https://doi.org:10.1038/s41388-019-0765-y
35 Tan, H. X. *et al.* TGFβ1 is essential for MSCs-CAFs differentiation and promotes HCT116 cells migration and invasion via JAK/STAT3 signaling. *Onco Targets Ther* **12**, 5323-5334 (2019). https://doi.org:10.2147/OTT.S178618
36 Zeisberg, E. M., Potenta, S., Xie, L., Zeisberg, M. & Kalluri, R. Discovery of endothelial to mesenchymal transition as a source for carcinoma-associated fibroblasts. *Cancer Res* **67**, 10123-10128 (2007). https://doi.org:10.1158/0008-5472.CAN-07-3127
37 Mao, X. *et al.* Crosstalk between cancer-associated fibroblasts and immune cells in the tumor microenvironment: new findings and future perspectives. *Mol Cancer* **20**, 131 (2021). https://doi.org:10.1186/s12943-021-01428-1
38 Kuzet, S. E. & Gaggioli, C. Fibroblast activation in cancer: when seed fertilizes soil. *Cell Tissue Res* **365**, 607-619 (2016). https://doi.org:10.1007/s00441-016-2467-x
39 Erez, N., Truitt, M., Olson, P., Arron, S. T. & Hanahan, D. Cancer-Associated Fibroblasts Are Activated in Incipient Neoplasia to Orchestrate Tumor-Promoting Inflammation in an NF-kappaB-Dependent Manner. *Cancer Cell* **17**, 135-147 (2010). https://doi.org:10.1016/j.ccr.2009.12.041
40 Biffi, G. *et al.* IL1-Induced JAK/STAT Signaling Is Antagonized by TGFβ to Shape CAF Heterogeneity in Pancreatic Ductal Adenocarcinoma. *Cancer Discov* **9**, 282-301 (2019). https://doi.org:10.1158/2159-8290.CD-18-0710
41 Sanz-Moreno, V. *et al.* ROCK and JAK1 signaling cooperate to control actomyosin contractility in tumor cells and stroma. *Cancer Cell* **20**, 229-245 (2011). https://doi.org:10.1016/j.ccr.2011.06.018
42 Ringuette Goulet, C. *et al.* Exosomes Induce Fibroblast Differentiation into Cancer-Associated Fibroblasts through TGFβ Signaling. *Mol Cancer Res* **16**, 1196-1204 (2018). https://doi.org:10.1158/1541-7786.MCR-17-0784
43 Yoshida, G. J. Regulation of heterogeneous cancer-associated fibroblasts: the molecular pathology of activated signaling pathways. *J Exp Clin Cancer Res* **39**, 112 (2020). https://doi.org:10.1186/s13046-020-01611-0
44 Tommelein, J. *et al.* Radiotherapy-Activated Cancer-Associated Fibroblasts Promote Tumor Progression through Paracrine IGF1R Activation. *Cancer Res* **78**, 659-670 (2018). https://doi.org:10.1158/0008-5472.CAN-17-0524

45 Wu, F. *et al.* Signaling pathways in cancer-associated fibroblasts and targeted therapy for cancer. *Signal Transduct Target Ther* **6**, 218 (2021). https://doi.org:10.1038/s41392-021-00641-0
46 Prakash, J. Cancer-Associated Fibroblasts: Perspectives in Cancer Therapy. *Trends Cancer* **2**, 277-279 (2016). https://doi.org:10.1016/j.trecan.2016.04.005
47 Louault, K., Li, R. R. & DeClerck, Y. A. Cancer-Associated Fibroblasts: Understanding Their Heterogeneity. *Cancers (Basel)* **12** (2020). https://doi.org:10.3390/cancers12113108
48 Winkler, J., Abisoye-Ogunniyan, A., Metcalf, K. J. & Werb, Z. Concepts of extracellular matrix remodelling in tumour progression and metastasis. *Nat Commun* **11**, 5120 (2020). https://doi.org:10.1038/s41467-020-18794-x
49 Chen, Y., McAndrews, K. M. & Kalluri, R. Clinical and therapeutic relevance of cancer-associated fibroblasts. *Nat Rev Clin Oncol* **18**, 792-804 (2021). https://doi.org:10.1038/s41571-021-00546-5
50 Gonzalez-Avila, G. *et al.* Matrix metalloproteinases participation in the metastatic process and their diagnostic and therapeutic applications in cancer. *Crit Rev Oncol Hematol* **137**, 57-83 (2019). https://doi.org:10.1016/j.critrevonc.2019.02.010
51 Shimoda, M. *et al.* Loss of the Timp gene family is sufficient for the acquisition of the CAF-like cell state. *Nat Cell Biol* **16**, 889-901 (2014). https://doi.org:10.1038/ncb3021
52 Mohammadi, H. & Sahai, E. Mechanisms and impact of altered tumour mechanics. *Nat Cell Biol* **20**, 766-774 (2018). https://doi.org:10.1038/s41556-018-0131-2
53 Liu, Q., Luo, Q., Ju, Y. & Song, G. Role of the mechanical microenvironment in cancer development and progression. *Cancer Biol Med* **17**, 282-292 (2020). https://doi.org:10.20892/j.issn.2095-3941.2019.0437
54 Gaggioli, C. *et al.* Fibroblast-led collective invasion of carcinoma cells with differing roles for RhoGTPases in leading and following cells. *Nat Cell Biol* **9**, 1392-1400 (2007). https://doi.org:10.1038/ncb1658
55 Hooper, S., Gaggioli, C. & Sahai, E. A chemical biology screen reveals a role for Rab21-mediated control of actomyosin contractility in fibroblast-driven cancer invasion. *Br J Cancer* **102**, 392-402 (2010). https://doi.org:10.1038/sj.bjc.6605469
56 Malanchi, I. *et al.* Interactions between cancer stem cells and their niche govern metastatic colonization. *Nature* **481**, 85-89 (2011). https://doi.org:10.1038/nature10694
57 Oskarsson, T. *et al.* Breast cancer cells produce tenascin C as a metastatic niche component to colonize the lungs. *Nat Med* **17**, 867-874 (2011). https://doi.org:10.1038/nm.2379
58 Scherz-Shouval, R. *et al.* The reprogramming of tumor stroma by HSF1 is a potent enabler of malignancy. *Cell* **158**, 564-578 (2014). https://doi.org:10.1016/j.cell.2014.05.045
59 Ren, Y. *et al.* Paracrine and epigenetic control of CAF-induced metastasis: the role of HOTAIR stimulated by TGF-ß1 secretion. *Mol Cancer* **17**, 5 (2018). https://doi.org:10.1186/s12943-018-0758-4
60 Tang, X. *et al.* Autocrine TGF-β1/miR-200s/miR-221/DNMT3B regulatory loop maintains CAF status to fuel breast cancer cell proliferation. *Cancer Lett* **452**, 79-89 (2019). https://doi.org:10.1016/j.canlet.2019.02.044
61 Straussman, R. *et al.* Tumour micro-environment elicits innate resistance to RAF inhibitors through HGF secretion. *Nature* **487**, 500-504 (2012). https://doi.org:10.1038/nature11183
62 Wang, L. *et al.* CAFs enhance paclitaxel resistance by inducing EMT through the IL-6/JAK2/STAT3 pathway. *Oncol Rep* **39**, 2081-2090 (2018). https://doi.org:10.3892/or.2018.6311

63 Calon, A. *et al.* Dependency of colorectal cancer on a TGF-β-driven program in stromal cells for metastasis initiation. *Cancer Cell* **22**, 571-584 (2012). https://doi.org:10.1016/j.ccr.2012.08.013
64 Peña, C. *et al.* STC1 expression by cancer-associated fibroblasts drives metastasis of colorectal cancer. *Cancer Res* **73**, 1287-1297 (2013). https://doi.org:10.1158/0008-5472.CAN-12-1875
65 Orimo, A. *et al.* Stromal fibroblasts present in invasive human breast carcinomas promote tumor growth and angiogenesis through elevated SDF-1/CXCL12 secretion. *Cell* **121**, 335-348 (2005). https://doi.org:10.1016/j.cell.2005.02.034
66 Sazeides, C. & Le, A. Metabolic Relationship Between Cancer-Associated Fibroblasts and Cancer Cells. *Adv Exp Med Biol* **1311**, 189-204 (2021). https://doi.org:10.1007/978-3-030-65768-0_14
67 Guido, C. *et al.* Metabolic reprogramming of cancer-associated fibroblasts by TGF-β drives tumor growth: connecting TGF-β signaling with "Warburg-like" cancer metabolism and L-lactate production. *Cell Cycle* **11**, 3019-3035 (2012). https://doi.org:10.4161/cc.21384
68 Martinez-Outschoorn, U. E., Lisanti, M. P. & Sotgia, F. Catabolic cancer-associated fibroblasts transfer energy and biomass to anabolic cancer cells, fueling tumor growth. *Semin Cancer Biol* **25**, 47-60 (2014). https://doi.org:10.1016/j.semcancer.2014.01.005
69 Zhang, D. *et al.* Metabolic reprogramming of cancer-associated fibroblasts by IDH3α downregulation. *Cell Rep* **10**, 1335-1348 (2015). https://doi.org:10.1016/j.celrep.2015.02.006
70 Jung, J. G. & Le, A. Targeting Metabolic Cross Talk Between Cancer Cells and Cancer-Associated Fibroblasts. *Adv Exp Med Biol* **1311**, 205-214 (2021). https://doi.org:10.1007/978-3-030-65768-0_15
71 Fu, Y. *et al.* The reverse Warburg effect is likely to be an Achilles' heel of cancer that can be exploited for cancer therapy. *Oncotarget* **8**, 57813-57825 (2017). https://doi.org:10.18632/oncotarget.18175
72 Sousa, C. M. *et al.* Pancreatic stellate cells support tumour metabolism through autophagic alanine secretion. *Nature* **536**, 479-483 (2016). https://doi.org:10.1038/nature19084
73 Chang, C. H. *et al.* Metabolic Competition in the Tumor Microenvironment Is a Driver of Cancer Progression. *Cell* **162**, 1229-1241 (2015). https://doi.org:10.1016/j.cell.2015.08.016
74 Meireson, A., Devos, M. & Brochez, L. IDO Expression in Cancer: Different Compartment, Different Functionality? *Front Immunol* **11**, 531491 (2020). https://doi.org:10.3389/fimmu.2020.531491
75 Niu, F. *et al.* Arginase: An emerging and promising therapeutic target for cancer treatment. *Biomed Pharmacother* **149**, 112840 (2022). https://doi.org:10.1016/j.biopha.2022.112840
76 Fearon, D. T. The carcinoma-associated fibroblast expressing fibroblast activation protein and escape from immune surveillance. *Cancer Immunol Res* **2**, 187-193 (2014). https://doi.org:10.1158/2326-6066.CIR-14-0002
77 Ruhland, M. K. *et al.* Stromal senescence establishes an immunosuppressive microenvironment that drives tumorigenesis. *Nat Commun* **7**, 11762 (2016). https://doi.org:10.1038/ncomms11762
78 De Jaeghere, E. A., Denys, H. G. & De Wever, O. Fibroblasts Fuel Immune Escape in the Tumor Microenvironment. *Trends Cancer* **5**, 704-723 (2019). https://doi.org:10.1016/j.trecan.2019.09.009

79 Cheng, Y. *et al.* Cancer-associated fibroblasts induce PDL1+ neutrophils through the IL6-STAT3 pathway that foster immune suppression in hepatocellular carcinoma. *Cell Death Dis* **9**, 422 (2018). https://doi.org:10.1038/s41419-018-0458-4
80 Mace, T. A. *et al.* Pancreatic cancer-associated stellate cells promote differentiation of myeloid-derived suppressor cells in a STAT3-dependent manner. *Cancer Res* **73**, 3007-3018 (2013). https://doi.org:10.1158/0008-5472.CAN-12-4601
81 Bailey, S. R. *et al.* Th17 cells in cancer: the ultimate identity crisis. *Front Immunol* **5**, 276 (2014). https://doi.org:10.3389/fimmu.2014.00276
82 Lakins, M. A., Ghorani, E., Munir, H., Martins, C. P. & Shields, J. D. Cancer-associated fibroblasts induce antigen-specific deletion of CD8. *Nat Commun* **9**, 948 (2018). https://doi.org:10.1038/s41467-018-03347-0
83 Inoue, C. *et al.* PD-L1 Induction by Cancer-Associated Fibroblast-Derived Factors in Lung Adenocarcinoma Cells. *Cancers (Basel)* **11** (2019). https://doi.org:10.3390/cancers11091257
84 Monteran, L. & Erez, N. The Dark Side of Fibroblasts: Cancer-Associated Fibroblasts as Mediators of Immunosuppression in the Tumor Microenvironment. *Front Immunol* **10**, 1835 (2019). https://doi.org:10.3389/fimmu.2019.01835
85 Joshi, R. S. *et al.* The Role of Cancer-Associated Fibroblasts in Tumor Progression. *Cancers (Basel)* **13** (2021). https://doi.org:10.3390/cancers13061399
86 Mezheyeuski, A. *et al.* Fibroblasts in urothelial bladder cancer define stroma phenotypes that are associated with clinical outcome. *Sci Rep* **10**, 281 (2020). https://doi.org:10.1038/s41598-019-55013-0
87 Zhou, Z. *et al.* CAFs-derived MFAP5 promotes bladder cancer malignant behavior through NOTCH2/HEY1 signaling. *FASEB J* **34**, 7970-7988 (2020). https://doi.org:10.1096/fj.201902659R
88 Du, Y. *et al.* The cancer-associated fibroblasts related gene CALD1 is a prognostic biomarker and correlated with immune infiltration in bladder cancer. *Cancer Cell Int* **21**, 283 (2021). https://doi.org:10.1186/s12935-021-01896-x
89 Wang, L. *et al.* EMT- and stroma-related gene expression and resistance to PD-1 blockade in urothelial cancer. *Nat Commun* **9**, 3503 (2018). https://doi.org:10.1038/s41467-018-05992-x
90 Zhuang, J. *et al.* TGFβ1 secreted by cancer-associated fibroblasts induces epithelial-mesenchymal transition of bladder cancer cells through lncRNA-ZEB2NAT. *Sci Rep* **5**, 11924 (2015). https://doi.org:10.1038/srep11924
91 Goulet, C. R. *et al.* Cancer-associated fibroblasts induce epithelial-mesenchymal transition of bladder cancer cells through paracrine IL-6 signalling. *BMC Cancer* **19**, 137 (2019). https://doi.org:10.1186/s12885-019-5353-6
92 Long, X. *et al.* Cancer-associated fibroblasts promote cisplatin resistance in bladder cancer cells by increasing IGF-1/ERβ/Bcl-2 signalling. *Cell Death Dis* **10**, 375 (2019). https://doi.org:10.1038/s41419-019-1581-6
93 Chen, Z. *et al.* Single-cell RNA sequencing highlights the role of inflammatory cancer-associated fibroblasts in bladder urothelial carcinoma. *Nat Commun* **11**, 5077 (2020). https://doi.org:10.1038/s41467-020-18916-5
94 Fang, X. *et al.* Twist2 contributes to breast cancer progression by promoting an epithelial-mesenchymal transition and cancer stem-like cell self-renewal. *Oncogene* **30**, 4707-4720 (2011). https://doi.org:10.1038/onc.2011.181
95 Pan, H. & Reilly, M. P. A protective smooth muscle cell transition in atherosclerosis. *Nat Med* **25**, 1194-1195 (2019). https://doi.org:10.1038/s41591-019-0541-0
96 Mota, J. M. *et al.* Post-Sepsis State Induces Tumor-Associated Macrophage Accumulation through CXCR4/CXCL12 and Favors Tumor Progression in Mice. *Cancer Immunol Res* **4**, 312-322 (2016). https://doi.org:10.1158/2326-6066.CIR-15-0170

97 Bordignon, P. *et al.* Dualism of FGF and TGF-β Signaling in Heterogeneous Cancer-Associated Fibroblast Activation with ETV1 as a Critical Determinant. *Cell Rep* **28**, 2358-2372.e2356 (2019). https://doi.org:10.1016/j.celrep.2019.07.092
98 Talia, C., Connolly, L. & Fowler, P. A. The insulin-like growth factor system: A target for endocrine disruptors? *Environ Int* **147**, 106311 (2021). https://doi.org:10.1016/j.envint.2020.106311
99 Annunziata, M., Granata, R. & Ghigo, E. The IGF system. *Acta Diabetol* **48**, 1-9 (2011). https://doi.org:10.1007/s00592-010-0227-z
100 Cabail, M. Z. *et al.* The insulin and IGF1 receptor kinase domains are functional dimers in the activated state. *Nat Commun* **6**, 6406 (2015). https://doi.org:10.1038/ncomms7406
101 Hakuno, F. & Takahashi, S. I. IGF1 receptor signaling pathways. *J Mol Endocrinol* **61**, T69-T86 (2018). https://doi.org:10.1530/JME-17-0311
102 Allard, J. B. & Duan, C. IGF-Binding Proteins: Why Do They Exist and Why Are There So Many? *Front Endocrinol (Lausanne)* **9**, 117 (2018). https://doi.org:10.3389/fendo.2018.00117
103 Pollak, M. Insulin and insulin-like growth factor signalling in neoplasia. *Nat Rev Cancer* **8**, 915-928 (2008). https://doi.org:10.1038/nrc2536
104 Li, J., Choi, E., Yu, H. & Bai, X. C. Structural basis of the activation of type 1 insulin-like growth factor receptor. *Nat Commun* **10**, 4567 (2019). https://doi.org:10.1038/s41467-019-12564-0
105 Li, W. & Miller, W. T. Role of the activation loop tyrosines in regulation of the insulin-like growth factor I receptor-tyrosine kinase. *J Biol Chem* **281**, 23785-23791 (2006). https://doi.org:10.1074/jbc.M605269200
106 De Meyts, P. & Shymko, R. M. Timing-dependent modulation of insulin mitogenic versus metabolic signalling. *Novartis Found Symp* **227**, 46-57; discussion 57-60 (2000). https://doi.org:10.1002/0470870796.ch4
107 Jung, H. J. & Suh, Y. Regulation of IGF -1 signaling by microRNAs. *Front Genet* **5**, 472 (2014). https://doi.org:10.3389/fgene.2014.00472
108 Zhang, W. & Liu, H. T. MAPK signal pathways in the regulation of cell proliferation in mammalian cells. *Cell Res* **12**, 9-18 (2002). https://doi.org:10.1038/sj.cr.7290105
109 Guo, Y. J. *et al.* ERK/MAPK signalling pathway and tumorigenesis. *Exp Ther Med* **19**, 1997-2007 (2020). https://doi.org:10.3892/etm.2020.8454
110 Hemmings, B. A. & Restuccia, D. F. PI3K-PKB/Akt pathway. *Cold Spring Harb Perspect Biol* **4**, a011189 (2012). https://doi.org:10.1101/cshperspect.a011189
111 Manning, B. D. & Cantley, L. C. AKT/PKB signaling: navigating downstream. *Cell* **129**, 1261-1274 (2007). https://doi.org:10.1016/j.cell.2007.06.009
112 Loh, A. H. *et al.* Dissecting the PI3K Signaling Axis in Pediatric Solid Tumors: Novel Targets for Clinical Integration. *Front Oncol* **3**, 93 (2013). https://doi.org:10.3389/fonc.2013.00093
113 Le Roith, D., Bondy, C., Yakar, S., Liu, J. L. & Butler, A. The somatomedin hypothesis: 2001. *Endocr Rev* **22**, 53-74 (2001). https://doi.org:10.1210/edrv.22.1.0419
114 Lin-Su, K. & Wajnrajch, M. P. Growth Hormone Releasing Hormone (GHRH) and the GHRH Receptor. *Rev Endocr Metab Disord* **3**, 313-323 (2002). https://doi.org:10.1023/a:1020949507265
115 Kaplan, S. A. & Cohen, P. The somatomedin hypothesis 2007: 50 years later. *J Clin Endocrinol Metab* **92**, 4529-4535 (2007). https://doi.org:10.1210/jc.2007-0526
116 Lu, M., Flanagan, J. U., Langley, R. J., Hay, M. P. & Perry, J. K. Targeting growth hormone function: strategies and therapeutic applications. *Signal Transduct Target Ther* **4**, 3 (2019). https://doi.org:10.1038/s41392-019-0036-y

117 Caputo, M. *et al.* Regulation of GH and GH Signaling by Nutrients. *Cells* **10** (2021). https://doi.org:10.3390/cells10061376
118 Yakar, S. *et al.* Liver-specific igf-1 gene deletion leads to muscle insulin insensitivity. *Diabetes* **50**, 1110-1118 (2001). https://doi.org:10.2337/diabetes.50.5.1110
119 Wang, Y., Bikle, D. D. & Chang, W. Autocrine and Paracrine Actions of IGF-I Signaling in Skeletal Development. *Bone Res* **1**, 249-259 (2013). https://doi.org:10.4248/BR201303003
120 Sjögren, K., Jansson, J. O., Isaksson, O. G. & Ohlsson, C. A model for tissue-specific inducible insulin-like growth factor-I (IGF-I) inactivation to determine the physiological role of liver-derived IGF-I. *Endocrine* **19**, 249-256 (2002). https://doi.org:10.1385/ENDO:19:3:249
121 Hellström, A. *et al.* Role of Insulinlike Growth Factor 1 in Fetal Development and in the Early Postnatal Life of Premature Infants. *Am J Perinatol* **33**, 1067-1071 (2016). https://doi.org:10.1055/s-0036-1586109
122 Aguirre, G. A., González-Guerra, J. L., Espinosa, L. & Castilla-Cortazar, I. Insulin-Like Growth Factor 1 in the Cardiovascular System. *Rev Physiol Biochem Pharmacol* **175**, 1-45 (2018). https://doi.org:10.1007/112_2017_8
123 García-Fernández, M. *et al.* Antioxidant effects of insulin-like growth factor-I (IGF-I) in rats with advanced liver cirrhosis. *BMC Gastroenterol* **5**, 7 (2005). https://doi.org:10.1186/1471-230X-5-7
124 García-Fernández, M., Delgado, G., Puche, J. E., González-Barón, S. & Castilla Cortázar, I. Low doses of insulin-like growth factor I improve insulin resistance, lipid metabolism, and oxidative damage in aging rats. *Endocrinology* **149**, 2433-2442 (2008). https://doi.org:10.1210/en.2007-1190
125 Pérez, R. *et al.* Mitochondrial protection by low doses of insulin-like growth factor- I in experimental cirrhosis. *World J Gastroenterol* **14**, 2731-2739 (2008). https://doi.org:10.3748/wjg.14.2731
126 Yakar, S., Werner, H. & Rosen, C. J. Insulin-like growth factors: actions on the skeleton. *J Mol Endocrinol* **61**, T115-T137 (2018). https://doi.org:10.1530/JME-17-0298
127 Yoshida, T. & Delafontaine, P. Mechanisms of IGF-1-Mediated Regulation of Skeletal Muscle Hypertrophy and Atrophy. *Cells* **9** (2020). https://doi.org:10.3390/cells9091970
128 Troncoso, R., Ibarra, C., Vicencio, J. M., Jaimovich, E. & Lavandero, S. New insights into IGF-1 signaling in the heart. *Trends Endocrinol Metab* **25**, 128-137 (2014). https://doi.org:10.1016/j.tem.2013.12.002
129 Smith, T. J. Insulin-like growth factor-I regulation of immune function: a potential therapeutic target in autoimmune diseases? *Pharmacol Rev* **62**, 199-236 (2010). https://doi.org:10.1124/pr.109.002469
130 Neirijnck, Y., Papaioannou, M. D. & Nef, S. The Insulin/IGF System in Mammalian Sexual Development and Reproduction. *Int J Mol Sci* **20** (2019). https://doi.org:10.3390/ijms20184440
131 Gurevich, E., Segev, Y. & Landau, D. Growth Hormone and IGF1 Actions in Kidney Development and Function. *Cells* **10** (2021). https://doi.org:10.3390/cells10123371
132 Kobeissy, F. H. (2015).
133 Heinen, A. *et al.* IGF1 Treatment Improves Cardiac Remodeling after Infarction by Targeting Myeloid Cells. *Mol Ther* **27**, 46-58 (2019). https://doi.org:10.1016/j.ymthe.2018.10.020
134 Aberg, N. D., Brywe, K. G. & Isgaard, J. Aspects of growth hormone and insulin-like growth factor-I related to neuroprotection, regeneration, and functional plasticity in

the adult brain. *ScientificWorldJournal* **6**, 53-80 (2006). https://doi.org:10.1100/tsw.2006.22
135 Hanahan, D. & Weinberg, R. A. The hallmarks of cancer. *Cell* **100**, 57-70 (2000). https://doi.org:10.1016/s0092-8674(00)81683-9
136 Lemmon, M. A. & Schlessinger, J. Cell signaling by receptor tyrosine kinases. *Cell* **141**, 1117-1134 (2010). https://doi.org:10.1016/j.cell.2010.06.011
137 Bähr, C. & Groner, B. The IGF-1 receptor and its contributions to metastatic tumor growth-novel approaches to the inhibition of IGF-1R function. *Growth Factors* **23**, 1-14 (2005). https://doi.org:10.1080/08977190400020229
138 Lodjak, J. & Verhulst, S. Insulin-like growth factor 1 of wild vertebrates in a life-history context. *Mol Cell Endocrinol* **518**, 110978 (2020). https://doi.org:10.1016/j.mce.2020.110978
139 Cevenini, A. *et al.* Molecular Signatures of the Insulin-like Growth Factor 1-mediated Epithelial-Mesenchymal Transition in Breast, Lung and Gastric Cancers. *Int J Mol Sci* **19** (2018). https://doi.org:10.3390/ijms19082411
140 Li, H. *et al.* IGF-IR signaling in epithelial to mesenchymal transition and targeting IGF-IR therapy: overview and new insights. *Mol Cancer* **16**, 6 (2017). https://doi.org:10.1186/s12943-016-0576-5
141 Yao, C. *et al.* IGF/STAT3/NANOG/Slug Signaling Axis Simultaneously Controls Epithelial-Mesenchymal Transition and Stemness Maintenance in Colorectal Cancer. *Stem Cells* **34**, 820-831 (2016). https://doi.org:10.1002/stem.2320
142 Li, H., Baldwin, B. R. & Zahnow, C. A. LIP expression is regulated by IGF-1R signaling and participates in suppression of anoikis. *Mol Cancer* **10**, 100 (2011). https://doi.org:10.1186/1476-4598-10-100
143 Zhang, Y. *et al.* Pan-Cancer Analysis of IGF-1 and IGF-1R as Potential Prognostic Biomarkers and Immunotherapy Targets. *Front Oncol* **11**, 755341 (2021). https://doi.org:10.3389/fonc.2021.755341
144 Lin, C. *et al.* Pre-diagnostic circulating insulin-like growth factor-I and bladder cancer risk in the European Prospective Investigation into Cancer and Nutrition. *Int J Cancer* **143**, 2351-2358 (2018). https://doi.org:10.1002/ijc.31650
145 Hua, H., Kong, Q., Yin, J., Zhang, J. & Jiang, Y. Insulin-like growth factor receptor signaling in tumorigenesis and drug resistance: a challenge for cancer therapy. *J Hematol Oncol* **13**, 64 (2020). https://doi.org:10.1186/s13045-020-00904-3
146 Osher, E. & Macaulay, V. M. Therapeutic Targeting of the IGF Axis. *Cells* **8** (2019). https://doi.org:10.3390/cells8080895
147 Puche, J. E. & Castilla-Cortázar, I. Human conditions of insulin-like growth factor-I (IGF-I) deficiency. *J Transl Med* **10**, 224 (2012). https://doi.org:10.1186/1479-5876-10-224
148 Ulanet, D. B., Ludwig, D. L., Kahn, C. R. & Hanahan, D. Insulin receptor functionally enhances multistage tumor progression and conveys intrinsic resistance to IGF-1R targeted therapy. *Proc Natl Acad Sci U S A* **107**, 10791-10798 (2010). https://doi.org:10.1073/pnas.0914076107
149 Seguin, L., Desgrosellier, J. S., Weis, S. M. & Cheresh, D. A. Integrins and cancer: regulators of cancer stemness, metastasis, and drug resistance. *Trends Cell Biol* **25**, 234-240 (2015). https://doi.org:10.1016/j.tcb.2014.12.006
150 Shin, D. H. *et al.* Combating resistance to anti-IGFR antibody by targeting the integrin β3-Src pathway. *J Natl Cancer Inst* **105**, 1558-1570 (2013). https://doi.org:10.1093/jnci/djt263
151 Shin, D. H. *et al.* Akt/mTOR counteract the antitumor activities of cixutumumab, an anti-insulin-like growth factor I receptor monoclonal antibody. *Mol Cancer Ther* **10**, 2437-2448 (2011). https://doi.org:10.1158/1535-7163.MCT-11-0235

152 Knowlden, J. M. *et al.* erbB3 recruitment of insulin receptor substrate 1 modulates insulin-like growth factor receptor signalling in oestrogen receptor-positive breast cancer cell lines. *Breast Cancer Res* **13**, R93 (2011). https://doi.org:10.1186/bcr3018
153 Yoon, S. O. *et al.* Focal Adhesion- and IGF1R-Dependent Survival and Migratory Pathways Mediate Tumor Resistance to mTORC1/2 Inhibition. *Mol Cell* **67**, 512-527.e514 (2017). https://doi.org:10.1016/j.molcel.2017.06.033
154 Ireland, L. *et al.* Chemoresistance in Pancreatic Cancer Is Driven by Stroma-Derived Insulin-Like Growth Factors. *Cancer Res* **76**, 6851-6863 (2016). https://doi.org:10.1158/0008-5472.CAN-16-1201
155 Lee, J. S. *et al.* STAT3-mediated IGF-2 secretion in the tumour microenvironment elicits innate resistance to anti-IGF-1R antibody. *Nat Commun* **6**, 8499 (2015). https://doi.org:10.1038/ncomms9499
156 Mutgan, A. C. *et al.* Insulin/IGF-driven cancer cell-stroma crosstalk as a novel therapeutic target in pancreatic cancer. *Mol Cancer* **17**, 66 (2018). https://doi.org:10.1186/s12943-018-0806-0
157 Šošić, D., Richardson, J. A., Yu, K., Ornitz, D. M. & Olson, E. N. Twist regulates cytokine gene expression through a negative feedback loop that represses NF-kappaB activity. *Cell* **112**, 169-180 (2003). https://doi.org:10.1016/s0092-8674(03)00002-3
158 Liu, J. P., Baker, J., Perkins, A. S., Robertson, E. J. & Efstratiadis, A. Mice carrying null mutations of the genes encoding insulin-like growth factor I (Igf-1) and type 1 IGF receptor (Igf1r). *Cell* **75**, 59-72 (1993).
159 Muzumdar, M. D., Tasic, B., Miyamichi, K., Li, L. & Luo, L. A global double-fluorescent Cre reporter mouse. *Genesis* **45**, 593-605 (2007). https://doi.org:10.1002/dvg.20335
160 Fantini, D. *et al.* A Carcinogen-induced mouse model recapitulates the molecular alterations of human muscle invasive bladder cancer. *Oncogene* **37**, 1911-1925 (2018). https://doi.org:10.1038/s41388-017-0099-6
161 Yu, Z. *et al.* Single-Cell Transcriptomic Map of the Human and Mouse Bladders. *J Am Soc Nephrol* **30**, 2159-2176 (2019). https://doi.org:10.1681/ASN.2019040335
162 Moulos, P. & Hatzis, P. Systematic integration of RNA-Seq statistical algorithms for accurate detection of differential gene expression patterns. *Nucleic Acids Res* **43**, e25 (2015). https://doi.org:10.1093/nar/gku1273
163 Werner, H. Insulin-Like Growth Factors in Development, Cancers and Aging. *Cells* **9** (2020). https://doi.org:10.3390/cells9102309